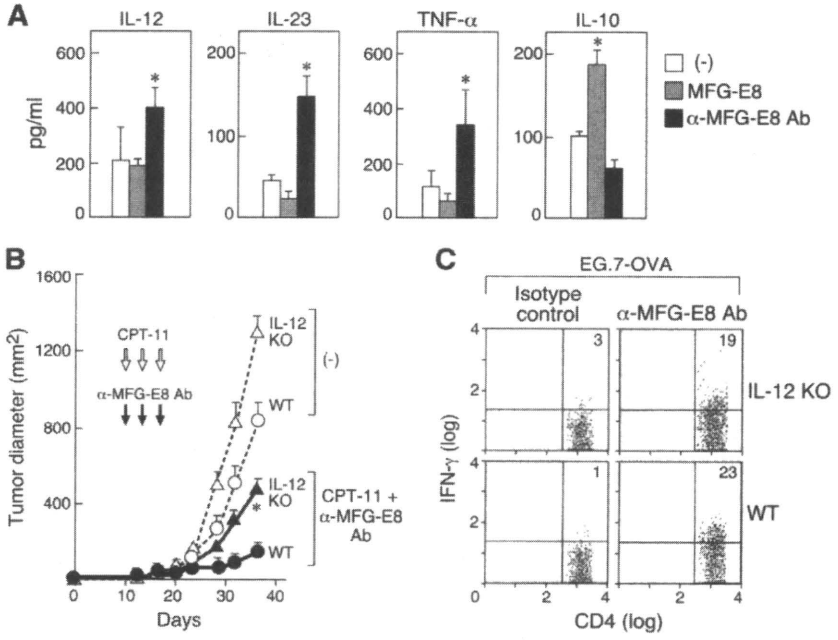


**Figure 6. Anti–MFG-E8 antibodies modulate antigen-presenting cell cytokine profiles.** (A) BMDCs were treated with recombinant MFG-E8 or anti–MFG-E8 mAbs, and cytokine production was determined with ELISA. Shown are the means ± SEM for three experiments. *, $P < 0.05$. (B) C57BL/6 wild-type or IL-12p35–deficient mice harboring established MC38 colon carcinomas (25 $mm^2$) were treated with systemic gemcitabine with or without anti–MFG-E8 mAb, as shown in Fig. 1 A. Shown are the means ± SEM for five mice per group. Similar results were observed in a second experiment. *, $P < 0.05$ between treated wild-type and IL-12 KO mice. (C) BMDCs from wild-type or IL-12–deficient mice were loaded with EG.7-OVA cells and co-cultured with $CD4^+$ T cells obtained from wild-type mice that were immunized with EG.7-OVA cells (five times). IFN-γ production was evaluated by flow cytometry (percentages are shown). Similar results were observed in a second experiment.

Recent work has illustrated that some cytotoxic therapies, including anthracyclines and taxanes, may induce a form of immunogenic cell death in which the release of calreticulin and high mobility group box 1 from dying tumor cells serves as an innate activating signal (34–36). Cytotoxic therapies may additionally trigger the DNA damage response to up-regulate tumor cell expression of NKG2D ligands, thereby eliciting NK and $CD8^+$ T cell responses (37). Moreover, agonistic antibodies to TNF-related apoptosis-inducing ligand receptors, which are frequently expressed on cancer cells, mediate potent antitumor effects in association with other immunotherapies (38, 39). Our results elucidate several novel antitumor mechanisms through which systemic MFG-E8 blockade may potentiate the efficacy of conventional oncologic therapies by coordinately targeting tumor cells and components of the tumor microenvironment. Perhaps the coupling of anti–MFG-E8 antibodies to tumor cell death might be considered a new strategy for in vivo cancer vaccination.

## MATERIALS AND METHODS

**Mice.** C57BL/6, NOD-SCID, and OVA transgenic OT-II mice were obtained from SRL or the Jackson Laboratory and housed under specific pathogen-free conditions. OT-I and IL-12p35 gene KO mice were used as previously described (40, 41). All experiments were conducted according to a protocol approved by the review committee of animal research at the Institute of Medical Sciences of the University of Tokyo or Keio University School of Medicine.

**In vivo tumor challenges.** 6-wk-old C57BL/6, NOD-SCID, or IL-12 KO female mice were injected intradermally with $10^5$ MC38 colon carcinoma, B16 melanoma, EL-4 thymoma, or MCA205 fibrosarcoma cells. After the tumors grew to an approximate size of 25 $mm^2$, the mice were treated with various therapeutic regimens. For the MC38 tumors, mice received on days 10, 12, and 14 1 or 4 mg/ml gemcitabine, 5 mg/ml 5-FU, 1 mg/ml CPT-11, 40 mg/ml of the VEGFR-2 mAb DC101 (ImClone Systems), or the 40 mg/ml of the EGFR tyrosine kinase inhibitor AG490 (MERCK). In some experiments, tumors were treated with five daily doses of irradiation (3 Gy at a rate of 4 Gy/min) using an isolator system. For the B16 tumors, mice were treated with 5 mg/ml doxorubicin, 2 mg/ml etoposide, or gemcitabine as described. For EL-4 thymoma cells, mice were treated with 5 mg/ml doxorubicin, as described. A hamster mAb against MFG-E8[1] (at 2 mg/ml; MBL International), an isotype control immunoglobulin IgG2a, or 1 mg/ml of rabbit polyclonal anti–MFG-E8 sera (provided by C. Thèry, Institut National de la Santé et de la Recherche Médicale, Paris, France) (17, 18) were administered concurrently with the cytotoxic therapies. In some studies, mice were also treated with depleting antibodies against CD4 (clone GK1.5), CD8 (clone 53-6.72), and NK1.1 (PK-136; American Type Culture Collection) at days −5, −3, and 0 relative to the cytotoxic therapy (40, 42). Tumor growth was monitored regularly and the products of the perpendicular diameters were recorded.

**Apoptosis assays.** Tumor cells were cultured in serum-free media and treated with various cytotoxic agents overnight with or without anti–MFG-E8 antibodies. To generate stable drug-resistant variants, MC38 cells were cultured in gradually increasing concentrations of gemcitabine (from 1 to 20 μg/ml) or CPT-11 (from 0.5 to 10 μg/ml) over ~8 wk. MFG-E8 expression was measured by flow cytometry using the hamster anti–MFG-E8 mAb followed by an anti–mouse IgG, as previously described (10). Secreted MFG-E8 levels

were measured with an ELISA according to the manufacture's instruction (R&D Systems). Cell death was determined with annexin V and propidium iodide staining, or DiOC6 labeling to quantify the mitochondrial membrane potential, according to the manufacturer's instructions (BD). To measure tumor apoptosis in vivo, we treated established MC38 or B16 tumors (25 $mm^2$) with 10 mg/ml gemcitabine or dacarbazine with or without anti–MFG-E8 antibodies, harvested the tumors 4 d after therapy, and measured caspase 3 activation in tumor homogenates with a colorimetric assay kit (Invitrogen).

**Immune assays.** Tumor-infiltrating lymphocytes were harvested with a cell gradient separation (Nocoprep; Axis-Shield), as previously described (10). Cell populations were characterized using mAbs against CD3, CD4, CD8, CD11b, CD11c, CD44, CD86, Gr-1, and Foxp3 (clone MF23). IFN-γ production was measured by intracellular flow cytometry, as previously described (10). Cytotoxicity was measured by incubating lymphoid cells isolated from draining lymph nodes with irradiated MC38 cells for 96 h and then testing lytic activity against $^{51}$Cr-labeled MC38 and B16 targets. The percent lysis was calculated as (experimental − spontaneous)/(maximum − spontaneous) × 100, using 5% Triton X and medium alone for determination of the maximum and spontaneous counts.

BMDCs were cultured from bone marrow precursors using GM-CSF–conditioned media for 7 d and were then treated with 100 ng/ml of recombinant MFG-E8 (R&D Systems), 20 μg/ml anti–MFG-E8 mAb (MBL International), or 20 μg/ml of polyclonal MFG-E8 antiserum overnight. Culture supernatants were evaluated for IL-12, IL-23, TNF-α, and IL-10 levels with ELISAs.

**Cross-priming assays.** Day 7 BMDCs were also co-cultured with irradiated EG.7-OVA cells (1:10 ratio) that were labeled with PKH26 (Sigma-Aldrich) in 12-well round-bottom plates, and phagocytosis was determined with flow cytometry. In some experiments, the tumor cells were pretreated with 30 mg/ml anti–MFG-E8 mAb for 30 min before the co-culture. The impact of blocking antibodies to $\alpha_v$ integrins (clone RMV-7; Millipore) or Fc receptors (clone 2.4G2; BD) on tumor cell uptake was similarly evaluated. To antigen presentation by DCs, naive $CD4^+$ T cells were isolated from the spleens of OT-I or OT-II mice by magnetic cell sorting (Miltenyi Biotec) and added to the tumor cell–loaded dendritic cells for 24 h. Intracellular IFN-γ expression in T cells was then determined by flow cytometry.

For in vivo cross-priming assays, $10^6$ irradiated EG.7-OVA cells per mouse were injected into the footpads of OT-I mice with 1 mg/ml anti–MFG-E8 mAb, 1 mg/ml anti-FcR blocking antibody (clone 2.4G2), or isotype control. 5 d after the challenge, mice were sacrificed, and the draining lymph node cells were isolated and cultured with 10 mg/ml MHC class I–restricted OVA peptides overnight. IFN-γ production by $CD8^+$ T cells was then determined by flow cytometry or ELISA using the culture supernatants.

**Statistical analysis.** Statistical analysis was performed using the unpaired Student's *t* test or one-way analysis of variance through all of the experimental procedures. Differences were considered significant when the p-value was $<0.05$.

**Online supplemental material.** Fig. S1 associates temporal relationships of anti–MFG-E8 antibody and chemotherapy administration in antitumor responses. Fig. S2 presents in vivo antitumor activities of anti–MFG-E8 antibody and doxorubicin against established EL-4 thymomas. Fig. S3 shows the humeral responses induced by in vivo treatment of anti–MFG-E8 antibody and chemotherapy. Fig. S4 shows the frequency of $CD11b^+$ and $CD11b^+$ Gr-$1^+$myelid cells at tumors with the treatments. Fig. S5 suggests the in vitro phagocytosis of apoptotic tumor cells by BMDCs. In Fig. S6, the effect of anti–MFG-E8 antibody was examined in mediating in vitro cross-presentation of OVA antigen to OT-I T cells by BMDCs. Online supplemental material is available at http://www.jem.org/cgi/content/full/jem.20082614/DC1.

We wish to thank Dr. Clotilde Théry for valuable advice in the making of rabbit polyclonal antibody against mouse MFG-E8; A. Kurose for her secretarial assistance; and S. Nakayama, A. Asami and R. Miyake for assistance with the in vivo tumor study, ELISA assay, and animal care. M. Jinushi, G. Dranoff, and H. Tahara were responsible for experimental design; M. Jinushi, M. Sato, and S. Nagai were responsible for the preparation and performance of experiments; data analysis and interpretation were performed by M. Jinushi, M. Sato, A. Kanamoto, A. Itoh, S. Nagai, S. Koyasu, G. Dranoff, and H. Tahara; and M. Jinushi, G. Dranoff, and H. Tahara prepared the manuscript.

This study was supported in part by the Grants-in-Aid for Scientific Research on Priority Areas (20015016 to H. Tahara) and for Young Scientists (Start-Up; 20890050 to M. Jinushi) from the Ministry of Education, Culture, Sports, Science and Technology of Japan, as well as by the Melanoma Research Alliance and the Research Foundation for the Treatment of Ovarian Cancer (G. Dranoff).

The authors have no conflicting financial interests.

**Submitted: 19 November 2008**
**Accepted: 17 April 2009**

## REFERENCES

1. Dranoff, G. 2004. Cytokines in cancer pathogenesis and cancer therapy. *Nat. Rev. Cancer.* 4:11–22.
2. de Visser, K.E., A. Eichten, and L.M. Coussens. 2006. Paradoxical roles of the immune system during cancer development. *Nat. Rev. Cancer.* 6:24–37.
3. Balkwill, F., K.A. Charles, and A. Mantovani. 2005. Smoldering and polarized inflammation in the initiation and promotion of malignant disease. *Cancer Cell.* 7:211–217.
4. Smyth, M.J., G.P. Dunn, and R.D. Schreiber. 2006. Cancer immunosurveillance and immunoediting: the roles of immunity in suppressing tumor development and shaping tumor immunogenicity. *Adv. Immunol.* 90:1–50.
5. Karin, M., and F.R. Greten. 2005. NF-kappaB: linking inflammation and immunity to cancer development and progression. *Nat. Rev. Immunol.* 5:749–759.
6. Yu, H., M. Kortylewski, and D. Pardoll. 2007. Crosstalk between cancer and immune cells: role of STAT3 in the tumour microenvironment. *Nat. Rev. Immunol.* 7:41–51.
7. Rakoff-Nahoum, S., and R. Medzhitov. 2007. Regulation of spontaneous intestinal tumorigenesis through the adaptor protein MyD88. *Science.* 317:124–127.
8. Naugler, W.E., T. Sakurai, S. Kim, S. Maeda, K. Kim, A.M. Elsharkawy, and M. Karin. 2007. Gender disparity in liver cancer due to sex differences in MyD88-dependent IL-6 production. *Science.* 317:121–124.
9. Jinushi, M., F.S. Hodi, and G. Dranoff. 2008. Enhancing the clinical activity of granulocyte-macrophage colony-stimulating factor-secreting tumor cell vaccines. *Immunol. Rev.* 222:287–298.
10. Jinushi, M., Y. Nakazaki, M. Dougan, D.R. Carrasco, M. Mihm, and G. Dranoff. 2007. MFG-E8 mediated uptake of apoptotic cells by APCs links the pro- and anti-inflammatory activities of GM-CSF. *J. Clin. Invest.* 117:1902–1913.
11. Hanayama, R., M. Tanaka, K. Miwa, A. Shinohara, A. Iwamatsu, and S. Nagata. 2002. Identification of a factor that links apoptotic cells to phagocytes. *Nature.* 417:182–187.
12. Jinushi, M., Y. Nakazaki, D.R. Carrasco, D. Draganov, N. Souders, M. Johnson, M.C. Mihm, and G. Dranoff. 2008. Milk fat globule EGF-8 promotes melanoma progression through coordinated Akt and Twist signaling in the tumor microenvironment. *Cancer Res.* 68:8889–8898.
13. Miller, A.J., and M.C. Mihm Jr. 2006. Melanoma. *N. Engl. J. Med.* 355:51–65.
14. Neutzner, M., T. Lopez, X. Feng, E.S. Bergmann-Leiner, W.W. Leiner, and M.C. Udey. 2007. MFG-E8/lactadherin promotes tumor growth in an angiogenesis-dependent transgenic mouse model of multistage carcinogenesis. *Cancer Res.* 67:6777–6785.
15. Carmon, L., I. Bobilev-Priel, B. Brenner, D. Bobilev, A. Paz, E. Bar-Haim, B. Tirosh, T. Klein, M. Fridkin, F. Lemonnier, et al. 2002. Characterization of novel breast carcinoma-associated BA46-derived peptides in HLA-A2.1/D(b)-beta2m transgenic mice. *J. Clin. Invest.* 110:453–462.
16. Meyerhardt, J. A., and R.J. Mayer. 2005. Systemic therapy for colorectal cancer. *N. Engl. J. Med.* 352:476–487.
17. Bu, H.F., X.L. Zuo, X. Wang, M.A. Ensslin, V. Koti, W. Hsueh, A.S. Raymond, B.D. Shur, and X.D. Tan. 2007. Milk fat globule-EGF factor8/lactadherin plays a crucial role in maintenance and repair of murine intestinal epithelium. *J. Clin. Invest.* 117:3673–3683.

18. Silvestre, J.S., C. Thery, G. Hamard, J. Boddaert, B. Aquilar, A. Delcayre, C. Houbron, R. Tamarat, O. Blanc-Brude, S. Heeneman, et al. 2005. Lactadherin promotes VEGF-dependent neovascularization. *Nat. Med.* 11:499–506.
19. Hanayama, R., M. Tanaka, K. Miyasaka, K. Aozasa, M. Koike, Y. Uchiyama, and S. Nagata. 2004. Autoimmune disease and impaired uptake of apoptotic cells in MFG-E8-deficient mice. *Science.* 304:1147–1150.
20. Miyasaka, K., R. Hanayama, M. Tanaka, and S. Nagata. 2004. Expression of milk fat globule epidermal growth factor 8 in immature dendritic cells for engulfment of apoptotic cells. *Eur. J. Immunol.* 34:1414–1422.
21. Kranich, J., N.J. Krautler, E. Heinen, M. Polymenidou, C. Bridel, A. Schildkecht, C. Huber, M.H. Kosco-Vibois, R. Zinkernagel, G. Miele, and A. Aquzzi. 2008. Follicular dendritic cells control engulfment of apoptotic bodies by secreting Mfge8. *J. Exp. Med.* 205:1293–1302.
22. Moore, M.W., F.R. Carbone, and M.J. Bevan. 1988. Introduction of soluble protein into the class I pathway of antigen processing and presentation. *Cell.* 54:777–785.
23. Murphy, K.M., A.B. Heimberger, and D.Y. Loh. 1990. Induction by antigen of intrathymic apoptosis of CD4+CD8+TCRlo thymocytes in vivo. *Science.* 250:1720–1723.
24. Kalergis, A.M., and J.V. Ravetch. 2002. Inducing tumor immunity through the selective engagement of activating Fcγ receptors on dendritic cells. *J. Exp. Med.* 195:1653–1659.
25. Coussens, L.M., and Z. Werb. 2002. Inflammation and cancer. *Nature.* 420:860–867.
26. Druker, B.J., and A. David. 2003. Karnofsky Award lecture. Imatinib as a paradigm of targeted therapies. *J. Clin. Oncol.* 21(23 Suppl.):239s–245s.
27. Ferrara, N. 2004. Vascular endothelial growth factor: basic science and clinical progress. *Endocr. Rev.* 25:581–611.
28. Rubin, R.H., and L.S. Young. 2002. Clinical Approach to Infection in the Compromised Host. Springer-Verlag New York Inc., New York. 100 pp.
29. Lacy-Hulbert, A., A.M. Smith, H. Tissire, M. Barry, D. Crowley, R.T. Bronson, J.T. Roes, J.S. Savill, and R.O. Hynes. 2007. Ulcerative colitis and autoimmunity induced by loss of myeloid alphav integrins. *Proc. Natl. Acad. Sci. USA.* 104:15823–15828.
30. Sosic, D., J.A. Richardson, K. Yu, D.M. Ornitz, and E.N. Olson. 2003. Twist regulates cytokine gene expression through a negative feedback loop that represses NF-kappaB activity. *Cell.* 112:169–180.
31. Dhodapkar, K.M., and M.V. Dhodapkar. 2005. Recruiting dendritic cells to improve antibody therapy of cancer. *Proc. Natl. Acad. Sci. USA.* 102:6243–6244.
32. Quezada, S.A., K.S. Peggs, M.A. Curran, and J.P. Allison. 2006. CTLA4 blockade and GM-CSF combination immunotherapy alters the intratumor balance of effector and regulatory T cells. *J. Clin. Invest.* 116:1935–1945.
33. Hodi, F.S., M. Butler, D.A. Oble, M.V. Seiden, F.G. Haluska, A. Kruse, S. Macrae, M. Nelson, C. Canning, I. Lowy, et al. 2008. Immunologic and clinical effects of antibody blockade of cytotoxic T lymphocyte-associated antigen 4 in previously vaccinated cancer patients. *Proc. Natl. Acad. Sci. USA.* 105:3005–3010.
34. Obeid, M., A. Tesniere, F. Ghiringhrlli, G.M. Fimia, L. Apetoh, J.L. Perfettini, M. Castedo, G. Miqnot, T. Panaretakis, N. Casares, et al. 2007. Calreticulin exposure dictates the immunogenicity of cancer cell death. *Nat. Med.* 13:54–61.
35. Apetoh, L., F. Ghiringhelli, A. Tesniere, M. Obeid, C. Ortiz, A. Criollo, G. Mignot, M.C. Maiuri, E. Ullrich, P. Saulnier, et al. 2007. Toll-like receptor 4-dependent contribution of the immune system to anticancer chemotherapy and radiotherapy. *Nat. Med.* 13:1050–1059.
36. Hynes, N.M., R.G. van der Most, R.A. Lake, and M.J. Smyth. 2008. Immunogenic anti-cancer chemotherapy as an emerging concept. *Curr. Opin. Immunol.* 20:545–557.
37. Gasser, S., and D.H. Raulet. 2006. The DNA damage response arouses the immune system. *Cancer Res.* 66:3959–3962.
38. Uno, T., K. Takeda, Y. Kojima, H. Yoshizawa, H. Akiba, R.S. Mittler, F. Geyjo, K. Okumura, H. Yagita, and M.J. Smyth. 2006. Eradication of established tumors in mice by a combination antibody-based therapy. *Nat. Med.* 12:693–698.
39. Johnstone, R.W., A.J. Fraw, and M.J. Smyth. 2008. The TRAIL apoptotic pathway in cancer onset, progression and therapy. *Nat. Rev. Cancer.* 8:782–798.
40. Kaiga, T., M. Sato, H. Kaneda, Y. Iwakura, T. Takayama, and H. Tahara. 2007. Systemic administration of Il-23 induces potent antitumor immunity primarily mediated through Th1-type response in association with the endogenously expressed IL-12. *J. Immunol.* 178:7571–7580.
41. Hogquist, K.A., S.C. Jameson, W.R. Heath, J.L. Howard, M.J. Bevan, and F.R. Carbone. 1994. T cell receptor antagonist peptides induce positive selection. *Cell.* 76:17–25.
42. Dranoff, G., E. Jaffee, A. Lazenby, P. Golumbek, H. Levitsky, K. Brose, V. Jackson, H. Hanada, D. Pardoll, and R.C. Mulligan. 1993. Vaccination with irradiated tumor cells engineered to secrete murine granulocyte-macrophage colony-stimulating factor stimulates potent, specific, and long-lasting anti-tumor immunity. *Proc. Natl. Acad. Sci. USA.* 90:3539–3543.

# Mammalian target of rapamycin and glycogen synthase kinase 3 differentially regulate lipopolysaccharide-induced interleukin-12 production in dendritic cells

Masashi Ohtani,[1,2] Shigenori Nagai,[1,2] Shuhei Kondo,[1] Shinta Mizuno,[1] Kozue Nakamura,[1] Masanobu Tanabe,[3] Tsutomu Takeuchi,[3] Satoshi Matsuda,[1,2] and Shigeo Koyasu[1,2]

[1]Department of Microbiology and Immunology, Keio University School of Medicine, Tokyo; [2]Core Research for Evolutional Science and Technology, Japan Science and Technology Agency, Saitama; and [3]Department of Tropical Medicine and Parasitology, Keio University School of Medicine, Tokyo, Japan

**Phosphoinositide 3-kinase (PI3K) negatively regulates Toll-like receptor (TLR)–mediated interleukin-12 (IL-12) expression in dendritic cells (DCs). We show here that 2 signaling pathways downstream of PI3K, mammalian target of rapamycin (mTOR) and glycogen synthase kinase 3 (GSK3), differentially regulate the expression of IL-12 in lipopolysaccharide (LPS)–stimulated DCs. Rapamycin, an inhibitor of mTOR, enhanced IL-12 production in LPS-stimulated DCs, whereas the activation of mTOR by lentivirus-mediated transduction of a constitutively active form of Rheb suppressed the production of IL-12. The inhibition of protein secretion or deletion of IL-10 cancelled the effect of rapamycin, indicating that mTOR regulates IL-12 expression through an autocrine action of IL-10. In contrast, GSK3 positively regulates IL-12 production through an IL-10–independent pathway. Rapamycin-treated DCs enhanced Th1 induction in vitro compared with untreated DCs. LiCl, an inhibitor of GSK3, suppressed a Th1 response on *Leishmania major* infection in vivo. These results suggest that mTOR and GSK3 pathways regulate the Th1/Th2 balance though the regulation of IL-12 expression in DCs. The signaling pathway downstream of PI3K would be a good target to modulate the Th1/Th2 balance in immune responses in vivo. (Blood. 2008; 112:635-643)**

## Introduction

Dendritic cells (DCs) recognize pathogens via pattern-recognition receptors, such as Toll-like receptors (TLRs), nucleotide-binding oligomerization domain (NOD)-like receptors, and retinoic acid inducible gene-1 (RIG-I)-like receptors, produce various cytokines, including interleukin-12 (IL-12), and thus activate the innate immune system, which in turn leads to the induction of adaptive immunity.[1-5] Bioactive IL-12 is composed of p40 and p35 subunits and functions as a crucial inducer of Th1 responses. IL-12 is typically produced by antigen-presenting cells such as DCs and monocytes-macrophages and plays an important role in infection and tumor immunity.[1-5] Because the overproduction of IL-12 gives rise to strong cell-mediated immunity and organ-specific autoimmune diseases via exaggerated Th1 cell differentiation, it is critical that IL-12 levels be tightly controlled.[5]

Phosphoinositide 3-kinases (PI3Ks) are lipid kinases playing important roles in various signal transduction pathways.[6] PI3K family members are classified into 4 subgroups according to their structure and substrate specificity. Among them, class IA heterodimeric PI3Ks are involved in receptor-mediated signaling pathways in the immune system.[6,7] Phosphatidylinositol-(3,4)bisphosphate and phosphatidylinositol(3,4,5)trisphosphate produced by class IA PI3Ks recruit specific signaling proteins containing a pleckstrin homology domain to the plasma membrane. These proteins include Akt and phosphoinositide-dependent kinase 1 and are involved in a wide range of cellular responses, such as cell growth, survival, and cytokine production.[6,7] PI3K signaling pathways are counteracted by phosphatase and tensin homologue deleted on chromosome 10 (PTEN), a 3-phosphoinositide–specific lipid phosphatase.[6]

We have previously demonstrated that PI3K negatively regulates IL-12 production in DCs stimulated with TLR ligands.[8,9] An enhanced Th1 response was observed on *Leishmania major* infection,[8] and an impaired Th2 response was observed on *Strongyloides venezuelensis* infection[10] in mice deficient for p85α, a major regulatory subunit of class IA PI3K, indicating that PI3K plays a key role in the regulation of Th1/ Th2 balance in vivo. Although several reports confirmed the negative feedback regulation of IL-12 production by PI3K on TLR stimulation,[11-13] the molecular mechanism(s) remains controversial.

One downstream substrate of PI3K pathways is a Ser/Thr protein kinase named "mammalian target of rapamycin" (mTOR), which regulates cell growth and protein synthesis by activating p70 S6 kinase (p70S6K) and by inhibiting eukaryotic initiation factor 4E-binding protein 1 (4E-BP1).[14] There are 2 functionally distinct mTOR complexes, mTORC1 and mTORC2, and only mTORC1 acts downstream of the PI3K-Akt-tuberous sclerosis complex 2 (TSC2)–Rheb signaling pathway to phosphorylate p70S6K and 4E-BP1 in a rapamycin-sensitive fashion[14] (Figure 1A). Although the mTOR pathway is activated in response to not only growth factors but also environmental stresses such as hypoxia,[14] the TLR-triggered mTOR function is poorly understood. In the present study, we show that mTOR negatively regulates IL-12 production through the production of IL-10 in DCs. We further demonstrate that glycogen synthase kinase 3 (GSK3), another downstream target of PI3K pathways, is also involved in the PI3K-mediated regulation of IL-12 production in a manner distinct from that of mTOR. We also provide evidence that the inhibition of mTOR and

Submitted February 1, 2008; accepted April 9, 2008. Prepublished online as *Blood* First Edition paper, May 20, 2008; DOI 10.1182/blood-2008-02-137430.

The online version of this article contains a data supplement.

The publication costs of this article were defrayed in part by page charge payment. Therefore, and solely to indicate this fact, this article is hereby marked "advertisement" in accordance with 18 USC section 1734.

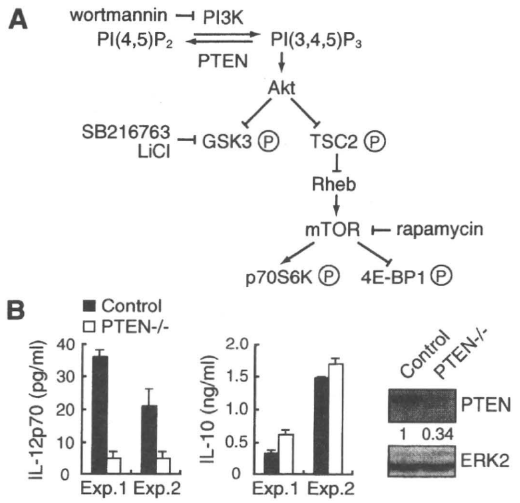


**Figure 1. LPS-induced IL-12 production is suppressed in PTEN$^{-/-}$ BMDCs.** (A) The overview of PI3K signaling pathway. $PI(4,5)P_2$ indicates phosphatidylinositol(4,5)bisphosphate; $PI(3,4,5)P_3$, phosphatidylinositol-(3,4,5)trisphosphate. (B) BMDCs from PTEN$^{-/-}$ mice (n = 2) or their littermate controls (n = 2) were stimulated with 1 μg/mL LPS for 24 hours and assayed for the production of IL-12p70 and IL-10 by ELISA. Data are indicated as median plus or minus SD. Essentially, the same results were obtained with 2 independent experiments (experiments 1 and 2). The expression levels of PTEN and ERK2 in BMDCs were determined by Western blotting (right panel).

GSK3 pathways in DCs results in the increase and decrease of Th1 responses, respectively.

## Methods

### Reagents

Lipopolysaccharide (LPS) from *Escherichia coli* 055:B5 was purchased from Sigma-Aldrich (St Louis, MO). Recombinant human (rh) GM-CSF, rhIL-4, rhIL-10, and recombinant mouse (rm) GM-CSF were purchased from PeproTech (Rocky Hill, NJ). Wortmannin, rapamycin, SB216763, cycloheximide, and brefeldin A (BFA) were purchased from Calbiochem (San Diego, CA). Antibodies to ERK2, IκBα, p70S6K, Rheb, GSK3α/β, and STAT3 were purchased from Santa Cruz Biotechnology (Santa Cruz, CA). Antibody to Akt and phosphorylation-specific antibodies to Akt (Ser473), GSK3α/β (Ser21/Ser9), TSC2 (Thr1462), p38 (Thr180/Tyr182), ERK (Thr202/Tyr204), JNK (Thr183/Tyr185), and STAT3 (Tyr705) were purchased from Cell Signaling Technology (Danvers, MA).

### Mice

C57BL/6 and BALB/c mice were purchased from Nihon SLC. IL-10$^{-/-}$ mice on a C57BL/6 background were purchased from The Jackson Laboratory (Bar Harbor, ME). Mice deficient for p85α were reported previously.[15,16] Mice had been backcrossed to the BALB/c background for 12 generations. STAT3 mutant (LysM-Cre x STAT3$^{flox/flox}$) mice[17] on a mixed (129 × C57BL/6) background were kindly provided by Dr K. Takeda (Osaka University, Osaka, Japan). STAT3$^{flox/flox}$ or LysM-Cre x STAT3$^{flox/+}$ mice were used as controls. PTEN mutant (LysM-Cre x PTEN$^{flox/flox}$) mice[18,19] on a C57BL/6 background were kindly provided by Dr A. Suzuki (Akita University, Akita, Japan). PTEN$^{flox/flox}$ mice were used as controls. LysM-Cre x STAT3$^{flox/flox}$ and LysM-Cre x PTEN$^{flox/flox}$ mice were referred to here as STAT3$^{-/-}$ and PTEN$^{-/-}$ mice, respectively. Mice were maintained at Taconic Farms (Germantown, NY) or in our animal facility under specific pathogen-free conditions. All experiments were performed in accordance with our institutional guidelines.

### Preparation of dendritic cells

To generate bone marrow (BM)–derived DCs (BMDCs), mouse BM cells were cultured at $10^6$/mL in complete medium (RPMI 1640; Sigma-Aldrich, 10% fetal calf serum, 55 μM 2-mercaptoethanol, 100 U/mL penicillin, 100 μg/mL streptomycin) supplemented with 10 ng/mL rmGM-CSF for 6 days. The culture medium was changed every 2 days. On day 6, BMDCs were isolated using antimouse CD11c magnetic beads (Miltenyi Biotec, Auburn, CA) with an AutoMACS (Miltenyi Biotec). Human peripheral blood mononuclear cells from normal healthy volunteers were isolated by centrifugation on a Ficoll-Metrizoate density gradient (Lymphoprep; Nycomed, Oslo, Norway). The protocol was approved by the local ethics committee at Keio University School of Medicine, and informed consent was obtained from donors in accordance with the Declaration of Helsinki. Monocytes were then isolated using antihuman CD14 magnetic beads (Miltenyi Biotec) with an AutoMACS, followed by incubation at $10^6$ cells/mL in complete medium supplemented with 100 ng/mL rhGM-CSF and 100 ng/mL rhIL-4 for 6 days, to obtain monocyte-derived DCs (MDDCs).

### Western blotting

Western blotting was carried out as described.[8] To detect phospho-STAT3 and phospho-TSC2, immunoreaction enhancer (Can Get Signal, Toyobo, Japan) was added to the reaction according to the manufacturer's instructions. ERK2 was used as a loading control. A LAS-3000 imaging system (Fuji) was used to produce digital images. Signal intensities (for phospho-STAT3) and signal profiles (for p70S6K) were quantified with Image Gauge software version 4.1 (Fuji).

### Enzyme-linked immunosorbent assay

Cytokine concentrations in the culture supernatants were quantified by enzyme-linked immunosorbent assay (ELISA; Quantikine; R&D Systems, Minneapolis, MN).

### Quantitative real-time polymerase chain reaction

Total RNA was prepared using NucleoSpin RNA II (Macherey-Nagel, Düreu, Germany), and cDNA was synthesized with Ready-To-Go T-Primed First-Strand kit (GE Healthcare, Chalfont St Giles, United Kingdom). Quantitative real-time polymerase chain reaction (PCR) was performed by applying the real-time SYBR Green PCR technology using SYBR premix Ex Taq (Takara, Otsu, Japan) with specific primers on an iCycler IQ (Bio-Rad, Hercules, CA). PCR cycling was as follows: 95°C for 10 seconds for 1 cycle, 95°C for 5 seconds, 58°C for 20 seconds, 72°C for 15 seconds for 40 cycles, and 70°C for 5 minutes. Amplification of cyclophilin A mRNA was done for each sample as an endogenous control. Primer pairs specific for IL-12p40 (forward, CAGAAGCTAACCATCTCCTGGTTTG; reverse, CCGGAGTAATTTGGTGCTCCACAC), IL-12p35 (forward, TCACATCTCATCTCCCCAAA; reverse, TCTGCTAACACATTGAGGGG), IL-10 (forward, GGTTGCC-AAGCCTTATCGGA; reverse, ACCTGCTCCACTGCCTTGCT), interferon-β (IFN-β) (forward, CCATCCAAGAGATGCTCCAG; reverse, GTGGAGAGCAGTTGAGGACA), suppressor of cytokine signaling 3 (SOCS3) (forward, GGGGGAGGCAGGAGGTGATGGA; reverse, GGGCGGGCTGGAGGTGGATT) and cyclophilin A (forward, ATGGCACTGGCGGCAGGTCC; reverse, TTGCCATTCCTGGACCCAAA) were used.

### Preparation of lentiviral vectors

The following constructs were kindly provided by Dr H. Miyoshi (RIKEN, Tsukuba, Japan): CSII-EF-MCS-IRES2-Venus, a self-inactivating lentiviral construct; pCAG-HIVgp and pCMV-VSVG-RSV-Rev, packaging constructs.[20] This lentiviral system is designed to express a desired gene under the direction of the elongation factor-1 promoter along with internal ribosomal entry site (IRES)-driven Venus, a derivative of YFP,[21] as a marker for monitoring the infection efficiency. Mouse Rheb was amplified by PCR using cDNA from the brain of C57BL/6 mice as a template (5′

primer, ATGCCTCAGTCCAAGTCCCG; 3′ primer, TCACATCACCGAGCACGAAG) and cloned into the pGEM-T Easy vector (Promega, Madison, WI). After sequence verification, the construct was subjected to PCR mutagenesis to obtain Rheb Q64L, a constitutively active form of Rheb, Glu-64 replaced by Leu. The product was verified by DNA sequencing and subcloned into CSII-EF-MCS-IRES2-Venus. For the generation of lentiviral vectors, 293T cells were transfected with CSII-EF-MCS-IRES2-Venus with or without Rheb Q64L insert, pCAG-HIVgp, and pCMV-VSUG-RSV-Rev using Lipofectamine 2000 (Invitrogen, Carlsbad, CA). After 2 days, culture supernatants were passed through a 0.45-μm filter, condensed to 0.5% volume, and used for gene transduction.

### Generation of gene-transduced BMDCs

Mouse BM cells were incubated with phycoerythrin-conjugated antibodies against CD3ε, CD4, CD8α, CD11b, Gr-1, B220, and TER119 (BD Biosciences, San Jose, CA) along with anti-phycoerythrin microbeads (Miltenyi Biotec), followed by negative selection with an AutoMACS. The remaining cells ($0.5 \times 10^5$ cells/0.5 mL) were cultured with 10 ng/mL rmGM-CSF in a 24-well plate for 2 days, followed by spin infection (1800 rpm, 2 hours) with 40 μL of each viral vector along with 5 μg/mL polybrene. After infection, each well was split into 2 wells (2 mL/well) and cultured with 10 ng/mL rmGM-CSF for another 4 days. The culture medium was changed every 2 days. The cells were then harvested, washed, and incubated with allophycocyanin-conjugated antimouse CD11c monoclonal antibody (mAb), and Venus-as well as CD11c-positive cells were sorted as gene-transduced BMDCs using a FACSAria (BD Biosciences). The purity was estimated to be more than 85%.

### $CD4^+$ T-cell priming

Human MDDCs ($1 \times 10^6$ cells) were incubated in the presence or absence of 10 μg/mL tuberculin purified protein derivative (PPD) for 1 hour, and subsequently stimulated with or without 1 μg/mL of LPS along with or without 100 nM of rapamycin. After 2 hours of stimulation, the cells were harvested, washed, and cultured ($3 \times 10^5$ cells) for a week with $CD4^+$ T cells from the same donor ($3 \times 10^6$ cells), which were isolated from peripheral blood mononuclear cells using antihuman CD4 magnetic beads (Miltenyi Biotec) with an AutoMACS. $CD4^+$ T cells were then restimulated with antihuman CD3ε (10 μg/mL) and antihuman CD28 (1 μg/mL) mAbs for 48 hours.

### *Leishmania major* infection

*L major* infection was performed as described.[8,22] Two days after infection, 40 μL of 2 mM LiCl/phosphate-buffered saline (PBS) or PBS were injected into the infected left hind footpad subcutaneously.

## Results

### Products of PI3K are involved in the regulation of IL-12 expression

To prove that the lipid kinase activity of PI3K regulates IL-12 production, we examined the role of PTEN, which catalyzes a reaction opposite to PI3K (Figure 1A). BMDCs lacking PTEN produced lower amounts of IL-12 than control BMDCs on LPS stimulation (Figure 1B), indicating that the products of PI3Ks, phosphatidylinositol(3,4,5)trisphosphate in particular, are indeed critical for the regulation of IL-12 expression.

### Activation of mTOR and GSK3 pathways by LPS stimulation of DCs

We examined the signaling components of PI3K-Akt pathway in LPS-stimulated BMDCs (Figure 1A). As shown in Figure 2, LPS stimulation induced the phosphorylation of TSC2 and GSK3,

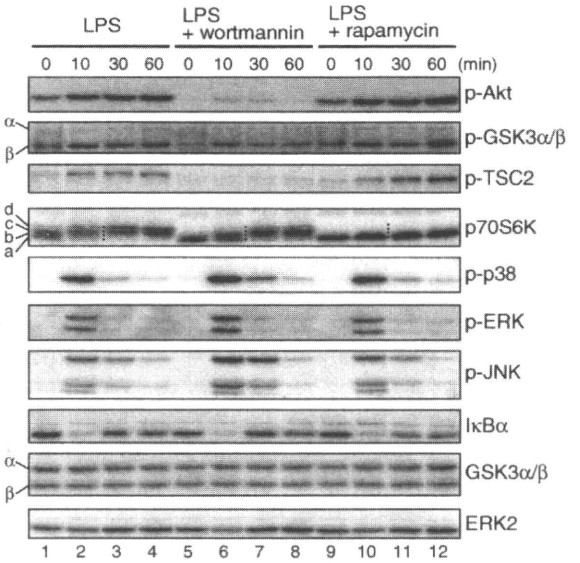


**Figure 2. The PI3K signaling pathway is activated by LPS in BMDCs.** BMDCs were cultured overnight and then pretreated with either 100 nM wortmannin or 10 ng/mL rapamycin for 20 minutes or left untreated before being stimulated with 1 μg/mL LPS for the indicated times. Cell lysates were analyzed for phospho-Akt, phospho-GSK3α/β, phospho-TSC2, p70S6K, phospho-p38, phospho-ERK, phospho-JNK, IκBα, GSK3α/β, and ERK2 by Western blotting. Four dots added between the 10-minute and 30-minute lanes of p70S6K samples indicate the migration positions of hyperphosphorylated p70S6K caused by multiple phosphorylation events, which are represented as a through d on the left side (Figure S1).

known targets of Akt. The activation of mTOR was evaluated by the phosphorylation of p70S6K. Consistent with the fact that mTOR is activated by serum and nutrients, p70S6K was partially phosphorylated even without LPS (Figure 2 lane 1). The hyperphosphorylation of p70S6K examined by electrophoretic mobility shifts was induced within 10 minutes (Figure 2 lane 2) and became clearer up to 60 minutes after LPS stimulation (Figure 2 and Figure S1 lane 4, available on the *Blood* website; see the Supplemental Materials link at the top of the online article; note that the electrophoretic mobility of p70S6K shifts from a and b up to c and d bands). Rapamycin completely blocked the phosphorylation of p70S6K (Figures 2, S1, compare lanes 1-4 and 9-12). In contrast, rapamycin had no effect on the LPS-induced phosphorylation of Akt and TSC2 (Figure 2 lanes 9-12), which is consistent with the fact that Akt and TSC2 act upstream of mTOR (Figure 1A). Wortmannin, an inhibitor of PI3K, only partially blocked the LPS-induced phosphorylation of p70S6K (Figures 2, S1, lanes 5-8), whereas the phosphorylation of Akt and TSC2 was completely inhibited (Figure 2 lanes 5-8). These data suggest that LPS-induced mTOR activation is mediated by both PI3K-dependent and-independent pathways, the latter of which could involve serum and/or nutrients.

GSK3 activity is negatively regulated by Akt-mediated phosphorylation.[23] We found that GSK3β was predominantly phosphorylated on LPS stimulation in BMDCs, whereas both GSK3α and GSK3β were expressed (Figure 2 lanes 1-4). The effect of wortmannin on GSK3β phosphorylation was partial (Figure 2 lanes 5-8), indicating that the LPS-induced phosphorylation of GSK3β was also mediated by both PI3K-dependent and -independent pathways. As expected, rapamycin had no effect on the LPS-induced phosphorylation of GSK3β (Figure 2 lanes 9-12).

We also examined the effects of rapamycin and wortmannin on LPS-activated MAPK and NF-κB pathways. Rapamycin had little effect on the phosphorylation status of MAPK family members or the degradation of IκBα, a measure of NF-κB activation (Figure 2, compare lanes 1-4 and lanes 9-12). In contrast, consistent with previous reports,[8,24,25] wortmannin slightly but reproducibly enhanced the LPS-induced phosphorylation of p38 as well as JNK (Figure 2, compare lanes 3 and 7), indicating that a PI3K-dependent but mTOR-independent pathway(s) negatively regulates the activation of p38 and JNK. Wortmannin had little effect on IκBα degradation, indicating that the NF-κB pathway is probably not the target of PI3K pathway in BMDCs.

### Rapamycin augments LPS-induced IL-12 production but suppresses IL-10 production in an mTOR-dependent manner

We next examined the role of mTOR in the regulation of IL-12 expression. As shown in Figure 3A, the treatment of BMDCs with rapamycin as well as wortmannin enhanced LPS-induced IL-12p70 production. In contrast, LPS-induced IL-10 production was suppressed by rapamycin or wortmannin, and the effect of rapamycin was more potent than wortmannin (Figure 3A). Rapamycin had the same effect on human MDDCs (Figure S2). On the other hand, rapamycin and wortmannin had little effect on the production of IL-6 and tumor necrosis factor-α (TNF-α; Figure 3A). PTEN$^{-/-}$ BMDCs produced slightly more IL-10 compared with control BMDCs (Figure 1B), but the effect of PTEN deficiency is more pronounced on IL-12 compared with IL-10 production.

A complex of rapamycin and FK506-binding protein 12 (FKBP12) binds to and inhibits mTOR. Because FK506 competes with rapamycin for binding to FKBP12, the excess amounts of FK506 cancel the biologic actions of the rapamycin-FKBP12 complex.[26] Indeed, FK506 prevented the rapamycin-induced augmentation of IL-12p70 and IL-12p40 production in a dose-dependent manner (Figure 3B). The suppression of IL-10 production by rapamycin was also canceled with excess FK506 (Figures 3B, S3). Excess amounts of FK506 partially restored the hyperphosphorylation of p70S6K (Figure S3). These results confirm that the effect of rapamycin on cytokine production is mediated by the inhibition of mTOR function.

We further examined the effects of wortmannin and rapamycin on LPS-induced cytokine mRNA expression, including IL-12p40, IL-12p35, IL-10, and IFN-β by real-time RT-PCR (Figure 3C). Consistent with these results, the expression of both IL-12p40 and IL-12p35 mRNAs was enhanced by wortmannin and rapamycin. In contrast, IL-10 mRNA expression was suppressed only by rapamycin. Interestingly, wortmannin but not rapamycin enhanced LPS-induced IFN-β mRNA expression. These results collectively suggest that the PI3K regulates the expression of distinct sets of cytokine genes expression in mTOR-dependent and -independent pathways.

### Constitutively active Rheb affects the regulation of cytokine production

To further confirm the role of mTOR in cytokine gene regulation, we used a lentiviral vector-mediated gene delivery system[20] to activate mTOR by expressing a constitutively active form of Rheb (Rheb Q64L).[27] The phosphorylation-induced electrophoretic mobility shift of p70S6K in untreated and LPS-stimulated DCs was augmented in BMDCs expressing Rheb Q64L compared with control BMDCs (Figure 4A and Figure S4 lanes 1 and 3, lanes 2 and 4), confirming the activity of Rheb Q64L. As shown in Figure

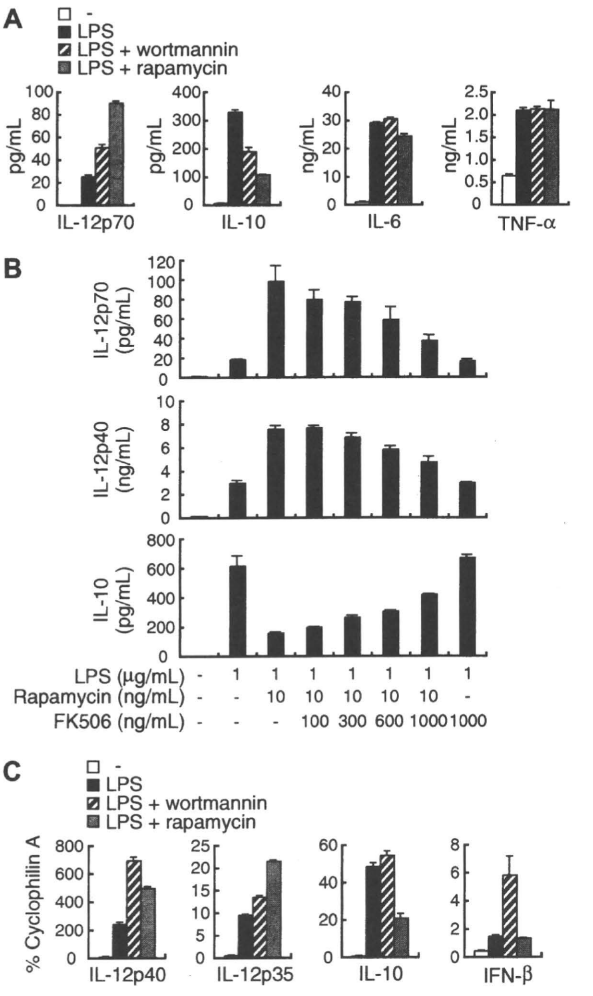


**Figure 3. The effect of rapamycin on LPS-induced cytokine expression in BMDCs.** (A) BMDCs were stimulated with 1 μg/mL LPS in the presence or absence of either 100 nM wortmannin or 10 ng/mL rapamycin for 24 hours and assayed for the production of IL-12p70, IL-10, IL-6, and TNF-α by ELISA. (B) BMDCs were stimulated with 1 μg/mL LPS with or without 10 ng/mL rapamycin along with the indicated concentrations of FK506 for 24 hours and assayed for the production of IL-12p70, IL-12p40, and IL-10 by ELISA. (C) BMDCs were pretreated with or without either 100 nM wortmannin or 10 ng/mL rapamycin for 20 minutes before stimulation with 1 μg/mL LPS. After 4 hours, total RNA was isolated, and IL-12p40, IL-12p35, IL-10, and IFN-β mRNA levels were assessed by real-time PCR using cyclophilin A mRNA as a reference. All data are indicated as median plus or minus SD of duplicate samples. Similar results were obtained with 2 to 4 independent experiments.

4B, LPS-induced IL-12p70 production was decreased in Rheb Q64L-expressing BMDCs compared with mock-infected BMDCs. In contrast, LPS-induced IL-10 production was increased in Rheb Q64L-expressing BMDCs. No difference in IL-6 production was observed (data not shown). These results indicate that mTOR is indeed involved in the regulation of IL-12 and IL-10 production in LPS-stimulated BMDCs.

### The effect of rapamycin on IL-12 expression involves IL-10 in an autocrine manner

Because mTOR is involved in diverse biologic processes, including protein synthesis and gene expression,[14] it is possible that mTOR regulates IL-12 gene expression through new protein synthesis. When BMDCs were treated with cycloheximide to inhibit de novo

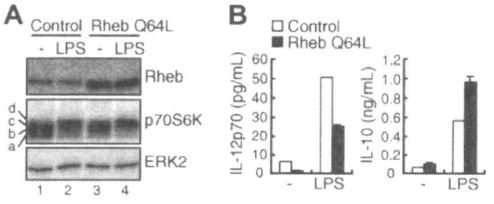


**Figure 4. The effect of Rheb Q64L on LPS-induced cytokine production.** BMDCs were infected with a lentivirus vector expressing a constitutively active form of Rheb (Rheb Q64L) or vector alone (control). Gene-transduced BMDCs were isolated ("Methods") and stimulated with or without 1 μg/mL LPS for 24 hours. (A) The cell lysates were analyzed for Rheb, p70S6K, and ERK2 by Western blotting. Note that the mobility shifts of p70S6K caused by multiple phosphorylation are represented as a through d (Figure S4). (B) The production of IL-12p70 and IL-10 in culture supernatants was assayed by ELISA.

protein synthesis, the effect of rapamycin was reduced (data not shown). BFA, which blocks protein secretion, abrogated the effect of rapamycin on LPS-induced IL-12p40 and IL-12p35 mRNA expression (Figure 5A). These results strongly suggest that rapamycin controls LPS-induced IL-12 expression through a newly synthesized autocrine mediator(s).

IL-10 is an anti-inflammatory cytokine capable of inhibiting the LPS-induced production of proinflammatory cytokines, including IL-12 in DCs.[28] When we examined the kinetics of LPS-induced IL-12 and IL-10 expression, rapamycin augmented IL-12p40 and IL-12p35 mRNA expression at 4 hours but not 2 hours after LPS stimulation (Figure 5B). On the other hand, the rapamycin-induced suppression of IL-10 mRNA expression was already observed at 2 hours after LPS stimulation (Figure 5B). Consistent with these results, LPS-induced IL-10 production evaluated by ELISA was significantly reduced by rapamycin at 4 hours after LPS stimulation, whereas IL-12p40 production was little affected (data not shown). These results suggest that the suppression of IL-10 expression by rapamycin subsequently augments IL-12 expression.

To test this hypothesis further, we examined whether rapamycin attenuates the IL-10 signaling pathway in LPS-stimulated DCs. For this purpose, we analyzed the phosphorylation status of STAT3 at Tyr705 as a measure of IL-10 signaling. We found that the tyrosine phosphorylation of STAT3 was markedly induced at 2 hours after LPS stimulation, which was inhibited by rapamycin (Figure 5C). Similar results were obtained in human MDDCs (Figure S5). To rule out the possibility that rapamycin directly inhibits the STAT3 signaling pathway, we examined the effect of rapamycin on the IL-10–induced expression of SOCS3, a well-known target of the STAT3 signaling pathway.[29] As shown in Figure 5D, SOCS3 mRNA expression induced by IL-10 stimulation was unaffected by rapamycin. Collectively, these results indicate that rapamycin directly suppresses LPS-induced IL-10 expression but not the STAT3 signaling pathway.

To confirm that rapamycin works through the IL-10-STAT3 pathway to down-regulate IL-12 expression, we used IL-10$^{-/-}$ and STAT3$^{-/-}$ DCs. As shown in Figure 5E, the effect of rapamycin was virtually absent in IL-10$^{-/-}$ BMDCs (1.2 ± 0.03-fold increase) compared with WT BMDCs (3.8 ± 0.1-fold increase). Essentially the same result was obtained with STAT3$^{-/-}$ BMDCs (Figure 5F, 3.3 ± 0.2-fold increase in control BMDCs vs 1.2 ± 0.1-fold increase in STAT3$^{-/-}$ BMDCs). The production of IL-12p70 from IL-10$^{-/-}$ DCs was strongly suppressed by the addition of exogenous IL-10, and such inhibition was rapamycin-independent (Figure S6). These results clearly indicate that rapamycin enhances IL-12 production through the inhibition of autocrine IL-10 action in LPS-stimulated BMDCs.

### mTOR and GSK3 cooperatively regulate LPS-induced IL-12 production

As wortmannin had only a marginal effect on LPS-induced phosphorylation of p70S6K (Figure 2) as well as IL-10 expression (Figure 3A,C), we examined pathways other than mTOR that lie downstream of PI3K. Indeed, GSK3 has been reported to regulate the TLR-mediated production of cytokines, such as IL-12p40 and IL-10 in human monocytes and DCs.[30,31] We therefore examined whether GSK3 regulates LPS-induced cytokine production in mouse BMDCs using SB216763, a specific GSK3 inhibitor. SB216763 attenuated IL-12p70 production but enhanced IL-10 production by LPS-stimulated DCs (Figure 6A, lane 5). We obtained similar results with another GSK3 inhibitor LiCl (data not shown). These data indicate that PI3K regulates IL-12 production through both mTOR and GSK3 pathways and that GSK3 positively regulates LPS-induced IL-12p70 and negatively regulates IL-10 production in BMDCs.

Given that the PI3K-Akt pathway negatively regulates GSK3 (Figure 1A), the treatment of cells with wortmannin should activate GSK3. Interestingly, wortmannin augmented the effect of rapamycin on LPS-induced IL-12p70 production (Figure 6A lanes 2-4 and 6). On the other hand, consistent with the marginal effect of wortmannin alone (Figure 6A lane 3), wortmannin failed to augment the suppressive effect of rapamycin on LPS-induced IL-10 production (Figure 6A lanes 2-4 and 6), suggesting that mTOR and GSK3 differentially regulate IL-12 production. Wortmannin had little effect on LPS-induced IL-12p70 and IL-10 production in the presence of SB216763 (Figure 6A lanes 5 and 7). It is probable that the contribution of GSK3 is similar to or greater than that of mTOR for the regulation of IL-12 production in DCs. Consistent with those observations, LPS-induced IL-12p70 production was decreased in the presence of SB216763 in IL-10$^{-/-}$ BMDCs (Figure 6B). These results collectively indicate that GSK3 directly regulates LPS-induced IL-12 production independent of IL-10 (Figure 6C).

### Attenuation of mTOR and GSK3 affects Th1/Th2 balance

Because IL-12 is critical for triggering Th1 responses, our results raise an interesting possibility that blocking mTOR and GSK3 may enhance and diminish Th1 responses, respectively. Human peripheral CD4$^+$ T cells stimulated with MDDCs pretreated with LPS plus PPD in the presence of rapamycin produced more IFN-γ on restimulation with anti-CD3 plus anti-CD28 antibodies than CD4$^+$ T cells stimulated with DCs pretreated in the absence of rapamycin (Figure 7A). It is thus probable that treatment of DCs with rapamycin results in the augmentation of a Th1 response presumably through enhanced IL-12 production and reduced IL-10 production. We next examined the effect of GSK3 inhibition in an in vivo infection model with *L major*, in which adequate Th1 development is required for disease control.[22] We have previously shown that Th2 prone BALB/c mice can elicit a reasonable Th1 response on *L major* infection in the absence of p85α (Fukao et al[8] and Figure 7B, compare open triangles and open circles). Because GSK3 is expected to have an increased activity in the absence of p85α, we administered a GSK3 inhibitor, LiCl, into footpad of p85α$^{-/-}$ mice on a BALB/c background when infected with *L major*. As shown in Figure 7B, whereas p85α$^{-/-}$ BALB/c mice were resistant to infection, the administration of LiCl to p85α$^{-/-}$ BALB/c mice resulted in increased footpad swelling and animals were no longer able to control the infection. These results

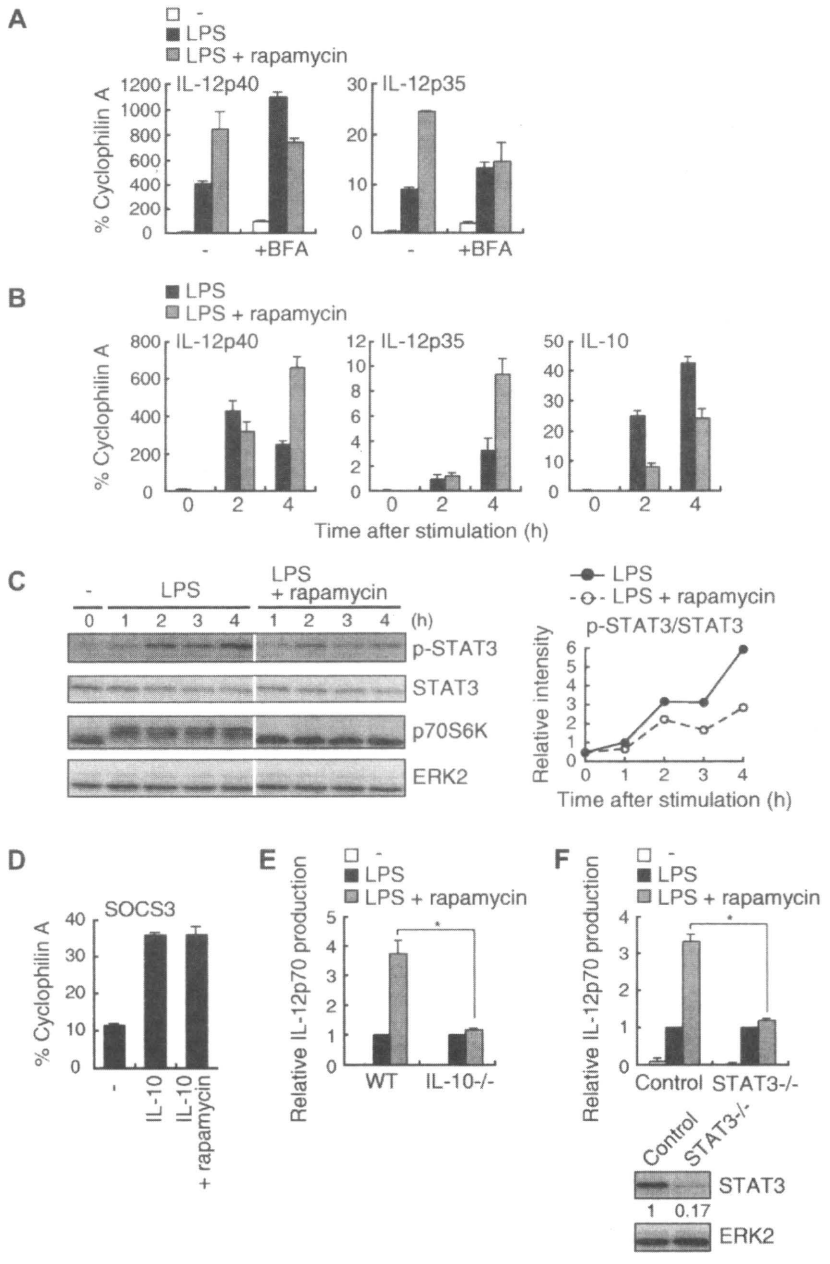


**Figure 5. The effect of rapamycin on LPS-induced IL-12 production depends on the IL-10–STAT3 signaling pathway.** (A) BMDCs were pretreated with or without 10 ng/mL rapamycin along with or without 5 μg/mL BFA for 20 minutes before stimulation with 1 μg/mL LPS. After 4 hours, total RNA was isolated, and IL-12p40 and IL-12p35 mRNA levels were assessed by real-time PCR using cyclophilin A mRNA as a reference. (B) BMDCs were pretreated with or without 10 ng/mL rapamycin for 20 minutes and then stimulated with 1 μg/mL LPS for the indicated times. Total RNA was isolated, and IL-12p40, IL-12p35, and IL-10 mRNA levels were assessed by real-time PCR using cyclophilin A mRNA as a reference. (C) BMDCs were pretreated with or without 100 ng/mL rapamycin for 20 minutes and then stimulated with 1 μg/mL LPS for the indicated times. The cell lysates were analyzed for phospho-STAT3, STAT3, p70S6K, and ERK2 by Western blotting. The white lines indicate that intervening lanes have been removed. The right panel indicates relative intensities of tyrosine-phosphorylated STAT3 normalized by STAT3 signals. (D) BMDCs were pretreated with or without 100 ng/mL rapamycin for 20 minutes before stimulation with 10 ng/mL IL-10. After 1 hour, total RNA was isolated, and SOCS3 mRNA levels were assessed by real-time PCR using cyclophilin A mRNA as a reference. In panels A, B, and D, data are indicated as mean plus or minus SD of duplicate samples. Data are representative of 2 (B,C) or 3 (A,D) independent experiments with similar results. (E) BMDCs from WT or IL-10$^{-/-}$ mice were stimulated with 1 μg/mL LPS in the presence or absence of 10 ng/mL rapamycin for 24 hours and assayed for the production of IL-12p70 by ELISA. Absolute IL-12p70 levels in the stimulation of LPS alone: WT, 24.1 plus or minus 3.6 pg/mL; IL-10$^{-/-}$, 1120 plus or minus 230 pg/mL. Data are indicated as median plus or minus SD of 3 independent experiments. *$P < .05$ by Mann-Whitney U test comparing WT with IL-10$^{-/-}$ groups. (F) BMDCs from STAT3$^{-/-}$ mice or littermate controls were stimulated with 0.1 μg/mL LPS in the presence or absence of 100 ng/mL rapamycin for 24 hours. Cytokine production was evaluated as in panel E. Absolute IL-12p70 levels in the stimulation of LPS alone: control, 11.8 plus or minus 3.7 pg/mL; STAT3$^{-/-}$, 299 plus or minus 67 pg/mL. *$P < .05$ by Mann-Whitney U test comparing control with STAT3$^{-/-}$ groups. Indicated below are the expression levels of STAT3 and ERK2 in BMDCs determined by Western blotting.

collectively indicate that the attenuation of mTOR and GSK3 by inhibitors affects the balance between Th1 and Th2 responses.

## Discussion

We have previously shown that PI3K negatively regulates TLR-induced pro-inflammatory cytokine production by DCs and gut epithelial cells.[8,9,25] Because LPS-induced IL-12 production was decreased in PTEN$^{-/-}$ BMDCs (Figure 1B), the PI3K-Akt pathway triggered by the lipid product of PI3K is indeed important for the suppression of LPS-induced IL-12 production.

Furthermore, our results show that the PI3K-Akt pathway positively regulates IL-10 production. IL-10 is produced by various cell types and plays anti-inflammatory roles in many immune responses.[32] In particular, it has been shown that DC-derived IL-10 is involved in a variety of responses, such as infectious diseases,[33] the induction of tolerance,[34] and cytotoxic T-lymphocyte–mediated antitumor activity.[32] Considering that IL-10 plays a pivotal role in immune regulation, the elucidation of the molecular mechanism underlying PI3K-mediated IL-10 regulation would shed new light on therapeutic approaches toward cancer as well as autoimmune diseases.

Indeed, signaling molecules involved in the PI3K pathway (ie, mTOR and GSK3) seem reasonable targets for appropriately modulating the Th1/Th2 balance. As shown here, the treatment of DCs with rapamycin augments a Th1 response (Figure 7A). Because rapamycin does not alter antigen uptake

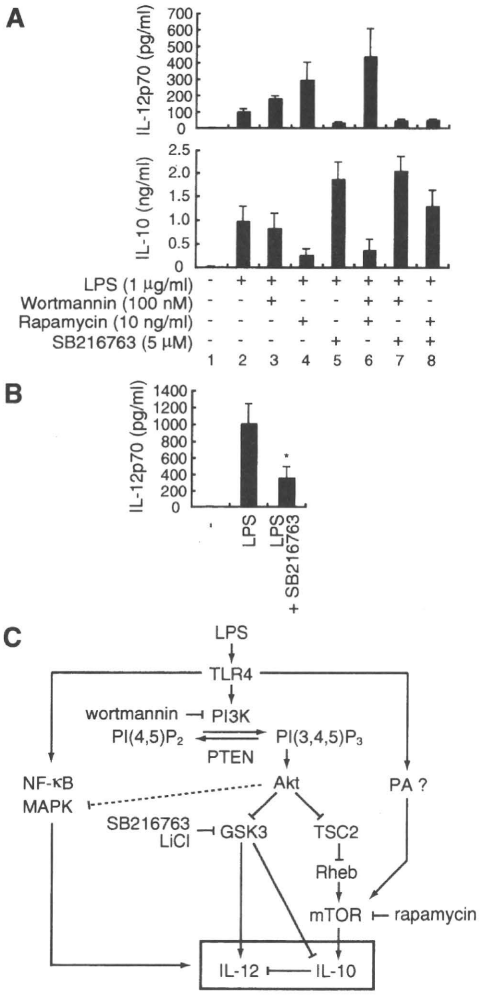


**Figure 6. mTOR and GSK3β regulate LPS-induced IL-12 production through distinct mechanisms.** (A) BMDCs were stimulated with 1 μg/mL LPS together with the indicated inhibitors for 24 hours and assayed for the production of IL-12p70 and IL-10 by ELISA. Data are indicated as median plus or minus SD of 3 independent experiments. (B) BMDCs from IL-10$^{-/-}$ mice were stimulated with 1 μg/mL LPS in the presence or absence of 5 μM SB216763 for 24 hours and assayed for the production of IL-12p70 by ELISA. Data are indicated as median plus or minus SD of 5 independent experiments. *$P < .05$ by Wilcoxon $t$ test compared with LPS alone. (C) The schematic diagram of the PI3K-mediated regulation of IL-12 production. PA indicates phosphatidic acid; $PI(4,5)P_2$, phosphatidylinositol(4,5)bisphosphate; $PI(3,4,5)P_3$, phosphatidylinositol(3,4,5)trisphosphate.

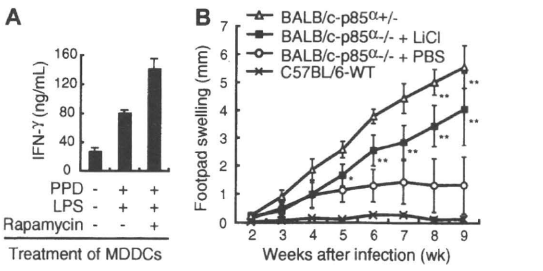


**Figure 7. The attenuation of mTOR and GSK3 affects Th1/Th2 balance.** (A) Human MDDCs were pretreated with PPD and LPS with or without rapamycin. CD4$^+$ T cells from the same donor were cultured with those MDDCs in the absence of rapamycin. After 1 week of incubation, CD4$^+$ T cells were stimulated with anti-CD3ε and anti-CD28 mAbs for 48 hours and assayed for the production of IFN-γ by ELISA. Data are indicated as median plus or minus SD of duplicate samples. (B) The footpad swelling of *L major*–infected BALB/c-p85α$^{-/-}$ mice treated with LiCl (n = 8) or with PBS (n = 6) was monitored on a weekly basis. BALB/c-p85α$^{+/-}$ mice (n = 5) or C57BL/6-WT mice (n = 2) were used as positive and negative controls for *L major* infection, respectively. Data are indicated as median plus or minus SD. *$P < .05$, **$P < .01$ by Mann-Whitney U test compared with PBS-treated BALB/c-p85α$^{-/-}$ mice. There was no significant difference in footpad swelling between LiCl-treated BALB/c-p85α$^{-/-}$ mice and untreated BALB/c-p85α$^{+/-}$ mice.

and presentation,[35] or the expression level of costimulatory molecules such as CD80 and CD86 in DCs,[36] the enhancement of a Th1 response by rapamycin is probably the result of the augmentation of IL-12 production. In addition, the inhibition of GSK3 by LiCl suppressed a Th1-mediated immune response against *L major* in vivo (Figure 7B). These results raise the possibility that the attenuation of these signaling pathways may provide new therapeutic approaches for human diseases.

Based on our present studies as well as other reports, we propose that signal transduction pathways downstream of Akt regulating IL-12 production are composed of at least 3 components: mTOR, GSK3, and MAPK (Figure 6C). First, the mTOR pathway negatively regulates IL-12 production through the induction of IL-10 gene expression. Wortmannin did not completely inhibit the LPS-induced phosphorylation of p70S6K (Figure 2), and a combination of wortmannin and rapamycin further enhanced LPS-induced IL-12 production (Figure 6A), suggesting that the LPS-induced mTOR activation depends only partially on the PI3K pathway. It should be noted that phosphatidic acid produced by LPS stimulation in macrophages activates mTOR in a PI3K-independent manner[37] (Figure 6C).

Second, the GSK3 pathway positively regulates IL-12 production in a more direct manner. Using human monocytes, Martin et al[30] showed that GSK3 positively regulates LPS-induced IL-12p40 production. GSK3 augments the binding of NF-κB p65 to a coactivator "cAMP response element-binding protein" (CREB)-binding protein by competitively inhibiting the binding of CREB to CREB-binding protein.[30] Rodionova et al[31] have also shown that GSK3 enhances IL-12p70 and IL-12p40 production by human *Escherichia coli*–activated MDDCs. Considering that the GSK3-mediated regulation of IL-12 production was independent of IL-10 (Figure 6B), it is probable that GSK3 controls LPS-induced IL-12 production by a mechanism distinct from mTOR.

Third and finally, we and others have reported that the treatment of monocytes or DCs with SB203580, a specific inhibitor of p38, suppressed LPS-induced IL-12 production.[8,11,38] In addition, consistent with the fact that Akt negatively regulates p38,[39] the inhibition of PI3K during LPS activation enhanced p38 phosphorylation and activation[8,24,25] (Figure 2). Conversely, p38 phosphorylation on LPS stimulation was decreased in macrophages derived from PTEN$^{-/-}$ mice.[40] These observations suggest that the PI3K-mediated suppression of p38 results in the attenuation of IL-12 production as well. It has also been reported that the PI3K-Akt pathway negatively regulates JNK activity.[41] Indeed, the treatment of BMDCs with wortmannin slightly enhanced LPS-induced JNK phosphorylation (Figure 2). Studies regarding the function of JNK in LPS-induced IL-12 production using human monocyte cell lines are controversial,[42,43] and the role of JNK in LPS-induced IL-12 production should be evaluated in primary cells, such as BMDCs derived from JNK-deficient mice. Given that rapamycin (Figure 2) and SB216763 (data not shown) had no effect on LPS-induced phosphorylation of p38 and JNK, it seems improbable that mTOR or GSK3 is involved in the PI3K-Akt pathway-mediated negative regulation of p38 and JNK activity. These results taken together indicate that mTOR, GSK3, and MAPK cooperatively regulate TLR-induced IL-12 production in DCs (Figure 6C).

In contrast to IL-10, IFN-β enhances IL-12 production in an autocrine manner.[44] Because wortmannin augments the expression of IFN-β in response to LPS (Figure 3C), it is possible that wortmannin enhances IL-12 production through IFN-β. However, whereas wortmannin enhances the expression of both IL-12p40 and IL-12p35, IFN-β enhances the expression of IL-12p35 but not IL-12p40,[44] suggesting that the effect of wortmannin is probably not mediated by IFN-β. In contrast to wortmannin, rapamycin affected only IL-10 but not IFN-β gene expression (Figure 3C).

Because IL-10 inhibits the LPS-induced production of a diverse array of cytokines, such as IL-6 and TNF-α in addition to IL-12,[28] rapamycin may influence the production of these cytokines. However, we found that rapamycin had no effect on LPS-induced IL-6 and TNF-α production (Figure 3A), consistent with a previous observation that the LPS-induced mRNA expression of IL-12p40, but not TNF-α, is decreased in BMDCs expressing a constitutively active STAT3.[45] Although not shown, rapamycin also augmented IL-12p40 production and suppressed IL-10 production in mouse BMDCs in response to other TLR ligands, such as zymosan (for TLR2/6) and CpG-ODN (for TLR9), whereas it had no effect on IL-6 production. It is possible that the expression of those cytokines has different sensitivities to the negative regulation by IL-10.

What is the molecular mechanism underlying the PI3K-mediated regulation of LPS-induced IL-10 production? p70S6K, one of the targets regulated by mTOR, is able to increase the translation of a subset of mRNAs that contain a 5′ tract of oligopyrimidine.[46] However, the 5′ tract of oligopyrimidine was not detected in mouse or human IL-10 mRNA. Another target molecule, 4E-BP1, regulates eIF-4E, which stimulates translational initiation but whose function is thought to be general and not restricted to a subset of genes. mTOR is also involved in gene transcription through the regulation of transcriptional factors without a translational event.[14,47,48] This mechanism is more probable because our observations indicate that rapamycin suppresses LPS-induced IL-10 production at a transcriptional level (Figure 3C), rather than through translational regulators. However, the DNA binding of transcriptional factor Sp1 to the *IL10* promoter in LPS-stimulated mice BMDCs was unaffected in the presence of rapamycin (data not shown). The regulation by transcription factors downstream of mTOR remains to be elucidated in future studies. In addition to mTOR, GSK3 is involved in a regulatory pathway for IL-10 production. Indeed, GSK3 negatively regulated LPS-induced IL-10 production (Figure 6A), presumably by inactivation of CREB,[30] which is involved in the transcriptional activation of the *IL10* gene.

It should be noted that many previous studies on the regulation of IL-10 or IL-12 gene expression were performed using macrophage or DC cell lines. We have been aware that cell lines and primary cells often showed different results. One obvious problem is the fact that many cell lines have some defect or alteration in PI3K-PTEN regulation, such that many immortalized cell lines lack PTEN expression and show enhanced Akt activity. These cells are obviously not suitable for studying PI3K pathways. Detailed analysis with primary cells is important in future studies.

## Acknowledgments

The authors thank Drs A. Suzuki, H. Miyoshi, and K. Takeda for valuable materials, Dr T. Luft of German Cancer Research Center for valuable discussion and sharing unpublished data, and Dr Linda K. Clayton of Harvard Medical School for critically reading the manuscript.

This work was supported by the Uehara Memorial Foundation, a Keio Gijuku Academic Development Fund (S. Matsuda), a Grant-in-Aid for Scientific Research (C 19590499; S. Matsuda) from the Japan Society for the Promotion of Science, a Grant-in-Aid for Scientific Research on Priority Areas (14021110 and 18073015), a National Grant-in-Aid for the Establishment of a High-Tech Research Center in a private university, and a Scientific Frontier Research Grant from the Ministry of Education, Culture, Sports, Science and Technology, Japan.

## Authorship

Contribution: M.O. designed the research, performed experiments, and wrote the paper; S.N., S. Kondo, S. Mizuno, K.N., and M.T. performed experiments; T.T. and S. Matsuda designed the research; and S. Koyasu designed the research and wrote the paper.

Conflict-of-interest disclosure: The authors declare no competing financial interests.

Correspondence: Shigeo Koyasu, Department of Microbiology and Immunology, Keio University School of Medicine, 35 Shinanomachi, Shinjuku-ku, Tokyo 160-8582, Japan; e-mail: koyasu@sc.itc.keio.ac.jp.

## References

1. Banchereau J, Briere F, Caux C, et al. Immunobiology of dendritic cells. Annu Rev Immunol. 2000; 18:767-811.
2. Steinman RM, Hemmi H. Dendritic cells: translating innate to adaptive immunity. Curr Top Microbiol Immunol. 2006;311:17-58.
3. Takeda K, Kaisho T, Akira S. Toll-like receptors. Annu Rev Immunol. 2003;21:335-376.
4. Creagh EM, O'Neill LA. TLRs, NLRs and RLRs: a trinity of pathogen sensors that co-operate in innate immunity. Trends Immunol. 2006;27:352-357.
5. Trinchieri G. Interleukin-12 and the regulation of innate resistance and adaptive immunity. Nat Rev Immunol. 2003;3:133-146.
6. Vanhaesebroeck B, Leevers SJ, Ahmadi K, et al. Synthesis and function of 3-phosphorylated inositol lipids. Annu Rev Biochem. 2001;70:535-602.
7. Koyasu S. The role of PI3K in immune cells. Nat Immunol. 2003;4:313-319.
8. Fukao T, Tanabe M, Terauchi Y, et al. PI3K-mediated negative feedback regulation of IL-12 production in DCs. Nat Immunol. 2002;3:875-881.
9. Fukao T, Koyasu S. PI3K and negative regulation of TLR signaling. Trends Immunol. 2003;24:358-363.
10. Fukao T, Yamada T, Tanabe M, et al. Selective loss of gastrointestinal mast cells and impaired immunity in PI3K-deficient mice. Nat Immunol. 2002;3:295-304.
11. Goodridge HS, Harnett W, Liew FY, Harnett MM. Differential regulation of interleukin-12 p40 and p35 induction via Erk mitogen-activated protein kinase-dependent and -independent mechanisms and the implications for bioactive IL-12 and IL-23 responses. Immunology. 2003;109:415-425.
12. Martin M, Schifferle RE, Cuesta N, Vogel SN, Katz J, Michalek SM. Role of the phosphatidylinositol 3 kinase-Akt pathway in the regulation of IL-10 and IL-12 by Porphyromonas gingivalis lipopolysaccharide. J Immunol. 2003;171:717-725.
13. Kuo CC, Lin WT, Liang CM, Liang SM. Class I and III phosphatidylinositol 3′-kinase play distinct roles in TLR signaling pathway. J Immunol. 2006; 176:5943-5949.
14. Wullschleger S, Loewith R, Hall MN. TOR signaling in growth and metabolism. Cell. 2006;124: 471-484.
15. Suzuki H, Terauchi Y, Fujiwara M, et al. Xid-like immunodeficiency in mice with disruption of the p85alpha subunit of phosphoinositide 3-kinase. Science. 1999;283:390-392.
16. Terauchi Y, Tsuji Y, Satoh S, et al. Increased insulin sensitivity and hypoglycaemia in mice lacking the p85 alpha subunit of phosphoinositide 3-kinase. Nat Genet. 1999;21:230-235.
17. Takeda K, Clausen BE, Kaisho T, et al. Enhanced Th1 activity and development of chronic enterocolitis in mice devoid of Stat3 in macrophages and neutrophils. Immunity. 1999; 10:39-49.
18. Clausen BE, Burkhardt C, Reith W, Renkawitz R,

Forster I. Conditional gene targeting in macrophages and granulocytes using LysMcre mice. Transgenic Res. 1999;8:265-277.

19. Suzuki A, Yamaguchi MT, Ohteki T, et al. T cell-specific loss of Pten leads to defects in central and peripheral tolerance. Immunity. 2001;14:523-534.
20. Miyoshi H, Blomer U, Takahashi M, Gage FH, Verma IM. Development of a self-inactivating lentivirus vector. J Virol. 1998;72:8150-8157.
21. Nagai T, Ibata K, Park ES, Kubota M, Mikoshiba K, Miyawaki A. A variant of yellow fluorescent protein with fast and efficient maturation for cell-biological applications. Nat Biotechnol. 2002;20:87-90.
22. Suzue K, Kobayashi S, Takeuchi T, Suzuki M, Koyasu S. Critical role of dendritic cells in determining the Th1/Th2 balance and the disease outcome upon *Leishmania major* infection. Int Immunol. 2008;20:337-343.
23. Cross DA, Alessi DR, Cohen P, Andjelkovich M, Hemmings BA. Inhibition of glycogen synthase kinase-3 by insulin mediated by protein kinase B. Nature. 1995;378:785-789.
24. Guha M, Mackman N. The phosphatidylinositol 3-kinase-Akt pathway limits lipopolysaccharide activation of signaling pathways and expression of inflammatory mediators in human monocytic cells. J Biol Chem. 2002;277:32124-32132.
25. Yu Y, Nagai S, Wu H, Neish AS, Koyasu S, Gewirtz AT. TLR5-mediated phosphoinositide 3-kinase activation negatively regulates flagellin-induced proinflammatory gene expression. J Immunol. 2006;176:6194-6201.
26. Bierer BE, Mattila PS, Standaert RF, et al. Two distinct signal transmission pathways in T lymphocytes are inhibited by complexes formed between an immunophilin and either FK506 or rapamycin. Proc Natl Acad Sci U S A. 1990;87:9231-9235.
27. Long X, Lin Y, Ortiz-Vega S, Yonezawa K, Avruch J. Rheb binds and regulates the mTOR kinase. Curr Biol. 2005;15:702-713.
28. Moore KW, de Waal Malefyt R, Coffman RL, O'Garra A. Interleukin-10 and the interleukin-10 receptor. Annu Rev Immunol. 2001;19:683-765.
29. Ding Y, Chen D, Tarcsafalvi A, Su R, Qin L, Bromberg JS. Suppressor of cytokine signaling 1 inhibits IL-10-mediated immune responses. J Immunol. 2003;170:1383-1391.
30. Martin M, Rehani K, Jope RS, Michalek SM. Toll-like receptor-mediated cytokine production is differentially regulated by glycogen synthase kinase 3. Nat Immunol. 2005;6:777-784.
31. Rodionova E, Conzelmann M, Maraskovsky E, et al. GSK-3 mediates differentiation and activation of proinflammatory dendritic cells. Blood. 2007; 109:1584-1592.
32. Mocellin S, Marincola FM, Young HA. Interleukin-10 and the immune response against cancer: a counterpoint. J Leukoc Biol. 2005;78:1043-1051.
33. McGuirk P, McCann C, Mills KH. Pathogen-specific T regulatory 1 cells induced in the respiratory tract by a bacterial molecule that stimulates interleukin 10 production by dendritic cells: a novel strategy for evasion of protective T helper type 1 responses by Bordetella pertussis. J Exp Med. 2002;195:221-231.
34. Akbari O, DeKruyff RH, Umetsu DT. Pulmonary dendritic cells producing IL-10 mediate tolerance induced by respiratory exposure to antigen. Nat Immunol. 2001;2:725-731.
35. Lee YR, Yang IH, Lee YH, et al. Cyclosporin A and tacrolimus, but not rapamycin, inhibit MHC-restricted antigen presentation pathways in dendritic cells. Blood. 2005;105:3951-3955.
36. Hackstein H, Taner T, Zahorchak AF, et al. Rapamycin inhibits IL-4-induced dendritic cell maturation in vitro and dendritic cell mobilization and function in vivo. Blood. 2003;101:4457-4463.
37. Foster DA. Regulation of mTOR by phosphatidic acid? Cancer Res. 2007;67:1-4.
38. Puig-Kroger A, Relloso M, Fernandez-Capetillo O, et al. Extracellular signal-regulated protein kinase signaling pathway negatively regulates the phenotypic and functional maturation of monocyte-derived human dendritic cells. Blood. 2001; 98:2175-2182.
39. Kim AH, Khursigara G, Sun X, Franke TF, Chao MV. Akt phosphorylates and negatively regulates apoptosis signal-regulating kinase 1. Mol Cell Biol. 2001;21:893-901.
40. Cao X, Wei G, Fang H, et al. The inositol 3-phosphatase PTEN negatively regulates Fc gamma receptor signaling, but supports Toll-like receptor 4 signaling in murine peritoneal macrophages. J Immunol. 2004;172:4851-4857.
41. Park HS, Kim MS, Huh SH, et al. Akt (protein kinase B) negatively regulates SEK1 by means of protein phosphorylation. J Biol Chem. 2002;277: 2573-2578.
42. Utsugi M, Dobashi K, Ishizuka T, et al. c-Jun N-terminal kinase negatively regulates lipopolysaccharide-induced IL-12 production in human macrophages: role of mitogen-activated protein kinase in glutathione redox regulation of IL-12 production. J Immunol. 2003;171:628-635.
43. Ma W, Gee K, Lim W, et al. Dexamethasone inhibits IL-12p40 production in lipopolysaccharide-stimulated human monocytic cells by down-regulating the activity of c-Jun N-terminal kinase, the activation protein-1, and NF-kappa B transcription factors. J Immunol. 2004;172:318-330.
44. Gautier G, Humbert M, Deauvieau F, et al. A type I interferon autocrine-paracrine loop is involved in Toll-like receptor-induced interleukin-12p70 secretion by dendritic cells. J Exp Med. 2005;201: 1435-1446.
45. Hoentjen F, Sartor RB, Ozaki M, Jobin C. STAT3 regulates NF-κB recruitment to the IL-12p40 promoter in dendritic cells. Blood. 2005;105: 689-696.
46. Jefferies HB, Fumagalli S, Dennis PB, Reinhard C, Pearson RB, Thomas G. Rapamycin suppresses 5'TOP mRNA translation through inhibition of p70s6k. EMBO J. 1997;16:3693-3704.
47. Soliman GA. The mammalian target of rapamycin signaling network and gene regulation. Curr Opin Lipidol. 2005;16:317-323.
48. Cunningham JT, Rodgers JT, Arlow DH, Vazquez F, Mootha VK, Puigserver P. mTOR controls mitochondrial oxidative function through a YY1-PGC-1alpha transcriptional complex. Nature. 2007; 450:736-740.

# ERK5 is involved in TCR-induced apoptosis through the modification of Nur77

**Yasushi Fujii[1,2], Satoshi Matsuda[1,3,a], Gensuke Takayama[1] and Shigeo Koyasu[1,3,*]**

[1]*Department of Microbiology and Immunology, Keio University School of Medicine, 35 Shinanomachi, Shinjuku-ku, Tokyo 160-8582, Japan*
[2]*Department of Pediatrics, Keio University School of Medicine, 35 Shinanomachi, Shinjuku-ku, Tokyo 160-8582, Japan*
[3]*Core Research for Evolutional Science and Technology, Japan Science and Technology Agency, Tokyo 102-0081, Japan*

**Nur77 is a nuclear orphan steroid receptor that has been implicated in negative selection when immature T cells are strongly activated through interaction with self peptide-MHC complexes. The expression of Nur77 in thymocytes and T cell lines leads to apoptosis in a manner dependent on its transcriptional activity. It is well established that Nur77 function is negatively regulated by post-translational modification. Here we demonstrate that the MAPK-induced phosphorylation of Nur77 during T cell activation plays a critical role in the induction of apoptosis. Upon T cell receptor (TCR) stimulation, ERK5 (also known as big MAP kinase 1, BMK1), a member of the MAPK family, phosphorylates Nur77, leading to its transcriptional activation. In contrast, the activation of the ERK2 signaling pathway failed to activate Nur77 although ERK2 is also able to phosphorylate Nur77. Furthermore, the blockade of ERK5 signaling pathway suppressed TCR-induced cell death. These results indicate that ERK5 regulates Nur77 function through its phosphorylation.**

## Introduction

Apoptosis or programmed cell death is essential for the development and homeostasis of T cells. In the thymus, $CD4^+CD8^+$ double positive (DP) thymocytes bearing T cell receptor (TCRs) that fail to recognize the self MHC molecules die rapidly through a process termed death by neglect, while the recognition of self MHC structures with bound peptide can trigger either functional differentiation (positive selection) or apoptosis (negative selection) of DP cells. If positively selected, immature DP thymocytes develop into mature single positive (SP) T cells expressing either CD4 or CD8. DP thymocytes bearing TCRs that strongly react with relatively abundant thymic self-antigens undergo negative selection, leading to the clonal deletion of potentially autoreactive T cells (von Boehmer 2004).

MAPK family members are evolutionarily conserved signaling molecules, which play a critical role in transducing extracellular signals to the nucleus. They include ERK1/2, JNKs, p38 MAPKs and ERK5 (also termed big MAP kinase 1, BMK1) (Nishida & Gotoh 1993; Cobb & Goldsmith 1995; Schaeffer & Weber 1999). These pathways have significant roles in mediating signals triggered by cytokines, growth factors and environmental stresses, and are involved in proliferation, differentiation and apoptosis in many cell types. Several studies have demonstrated that intracellular signals through different MAPK cascades selectively regulate T cell development in the thymus: the ERK1/2 pathway is involved in positive selection and the p38 and/or JNK pathways in negative selection (Rincon *et al.* 1998; Sugawara *et al.* 1998; Diehl *et al.* 2000). It has also been reported that the duration and strength of ERK1/2 activation regulate both positive and negative selection (Mariathasan *et al.* 2001). However, the molecular targets of MAPK cascades during thymic selection remain obscure.

Nur77 (also known as NGFI-B in rat and TR3 in human), an orphan nuclear steroid receptor, plays a critical role in negative selection (Winoto & Littman 2002; Hsu *et al.* 2004). The expression of a dominant-negative Nur77 blocks activation-induced cell death in T-cell hybridomas as well as negative selection in the thymus of transgenic mice (Zhou *et al.* 1996). Conversely, transgenic mice that express wild-type Nur77 exhibit enhanced apoptosis and a reduction in both thymocyte numbers

*Communicated by*: Eisuke Nishida
**Correspondence*: Email: koyasu@sc.itc.keio.ac.jp
[a]*Present address*: Department of Cell Signaling, Institute of Biomedical Science, Kansai Medical University, Moriguchi 570-8506, Japan

DOI: 10.1111/j.1365-2443.2008.01177.x

and the proportion of DP thymocytes (Calnan *et al.* 1995). Thus, Nur77 likely plays an important role in T cell apoptosis.

TCR-mediated Nur77 expression requires an increase in intracellular calcium concentration (Woronicz *et al.* 1995). The Nur77 promoter has two calcium-regulated consensus binding sites for myocyte enhancer factor-2 (MEF2) (Woronicz *et al.* 1995). These observations implicate MEF2, originally discovered as a transcription factor for muscle-specific gene expression, as a calcium-dependent transcription factor for Nur77 expression. Recent findings further indicate that a TCR-induced increase in intracellular calcium concentration leads to the dissociation of MEF2 from Cabin1 as a result of the competitive binding of activated calmodulin to Cabin1, resulting in MEF2 binding to the Nur77 promoter (Youn *et al.* 1999). In addition to the calcium–MEF2 pathway, MAPK signaling pathways are also involved in the induction of Nur77 in excitable cells such as muscle and nerve cells (van den Brink *et al.* 1999; Sakaue *et al.* 2001). It is thus likely that Nur77 function is regulated through a MAPK pathway in addition to the MEF2 pathway during TCR-mediated apoptosis.

Here we demonstrate that Nur77 is phosphorylated through the ERK5 pathway. It has been shown that Akt-mediated phosphorylation of Nur77 inhibits its DNA binding activity (Masuyama *et al.* 2001). In contrast, ERK5-mediated phosphorylation is indispensable for the positive regulation of Nur77 function, as the inhibition of ERK5 pathway results in the blockade of TCR-mediated apoptosis. These results indicate that ERK5 plays an essential role in TCR-mediated apoptosis presumably through the post-translational modification of Nur77.

## Results

### Regulation of Nur77 function through its phosphorylation

TCR stimulation results in the activation-induced cell death of a murine T-cell hybridoma, DO11.10 cells (Liu *et al.* 1994; Woronicz *et al.* 1994). The same stimulation induced the transient expression of Nur77 in these cells (Fig. 1A) (Winoto & Littman 2002; Hsu *et al.* 2004). Similar to TCR stimulation, simultaneous stimulation with PMA and A23187 that can mimic TCR signals (Koyasu *et al.* 1987) induced Nur77 expression, reaching a peak at 3 h after stimulation (data not shown). The stimulation of cells with A23187 alone induced the expression of Nur77 to a level comparable to PMA and A23187 stimulation while stimulation with PMA alone failed to induce Nur77 expression (Fig. 1B, upper panel).

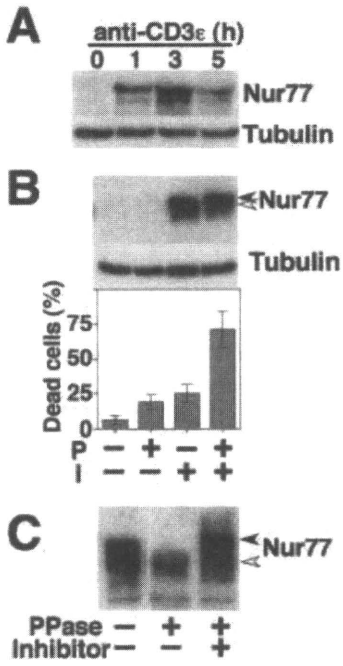


**Figure 1** Nur77 is phosphorylated during T cell activation. (A) DO11.10 cells were stimulated with plate-bound anti-CD3ε (145-2C11) mAb for the indicated times. Cell lysates (corresponding to $2 \times 10^6$ cells) were then obtained and subjected to immunoblot analysis with an anti-Nur77 mAb (upper panel) or an anti-α-tubulin mAb (lower panel) as a loading control. (B) DO11.10 cells were stimulated with 5 ng/mL PMA (P) and/or 200 ng/mL A23187 (I) and subjected to immunoblot analysis using the anti-Nur77 mAb (3 h after stimulation, upper panel) or the anti-αtubulin mAb as a loading control (middle panel) as well as cell death assay by a dye-exclusion method (20 h after stimulation, lower panel). As for death assay, three independent experiments were performed and data are presented as means ± SD. Closed and open arrowheads indicate Nur77 bands corresponding to a slower migrating form and a faster migrating form, respectively. (C) DO11.10 cells were stimulated with 5 ng/mL PMA and 200 ng/ml A23187 for 3 h. The cell lysates were obtained without phosphatase inhibitors, followed by incubation with 50 U/mL calf intestine alkaline phosphatase (PPase) in the presence or absence of 100 mM β-glycerophosphate (Inhibitor) at 37 °C for 30 min. Closed and open arrowheads indicate Nur77 bands corresponding to a phosphorylated form and a non-phosphorylated form, respectively.

This is in line with the previous observation that the expression level of Nur77 is regulated through the $Ca^{2+}$-induced Cabin1–MEF2 pathway (Youn *et al.* 1999). To our surprise, however, treatment with A23187 alone caused apoptosis in DO11.10 cells only marginally, whereas simultaneous stimulation with PMA was required

to fully induce apoptosis (Fig. 1B, lower panel). It should be noted that the electrophoretic mobility of Nur77 is somewhat slower when stimulated with PMA and A23187 compared to stimulation with A23187 alone (compare lanes 3 and 4), raising the possibility that the PMA-induced modification of Nur77 is involved in its ability to cause apoptosis. Given that the phosphorylation status of proteins often affects their electrophoretic mobility, we examined whether Nur77 is phosphorylated during T cell activation. Nur77 induced via simultaneous stimulation with PMA and A23187 was incubated with alkaline phosphatase in the presence or absence of a phosphatase inhibitor. Treatment with alkaline phosphatase resulted in the disappearance of the more slowly migrating Nur77 protein bands while the addition of a phosphatase inhibitor to the reaction canceled the effect of alkaline phosphatase (Fig. 1C). These results strongly suggest that Nur77 is phosphorylated during T cell activation presumably through PMA-sensitive signaling pathways.

### MAPK signaling pathway is responsible for Nur77 phosphorylation

Given that PMA treatment activates a variety of MAPK family members, we investigated the effects of MAPK inhibitors on PMA-induced Nur77 phosphorylation. Since p38 and/or JNK pathways are implicated in negative selection in the thymus (Rincon *et al.* 1998; Sugawara *et al.* 1998; Diehl *et al.* 2000), we initially expected that Nur77 phosphorylation would be suppressed in the presence of SB203580. Although SB203580 is a well-known inhibitor for p38, it has been reported that SB203580 is also able to inhibit JNK activity at a concentration higher than 10 μM (Chen *et al.* 1998). Contrary to our expectation, SB203580 had little effect on Nur77 phosphorylation during T cell activation (Fig. 2A). In contrast, the treatment of cells with PD98059 as well as U0126, both of which are well-known inhibitors for the ERK1/2 cascade (Pang *et al.* 1995; DeSilva *et al.* 1998), suppressed the phosphorylation of Nur77, which is demonstrated by disappearance of the slowly migrating bands (Fig. 2A).

As previously reported (Yazdanbakhsh *et al.* 1995), treatment with cyclosporin A (CsA), a potent inhibitor of the calcium–calcineurin pathway, led to the marked reduction of Nur77 expression (Fig. 2A). Interestingly, CsA had little effect on the phosphorylation status of Nur77 as demonstrated by the existence of the slowly migrating bands (Fig. 2B). At concentrations ranging from 2.5 to 10 μM, U0126 had, if any, a marginal effect on Nur77 expression while blocking Nur77 phosphorylation (Fig. 2B). However, Nur77 expression during T

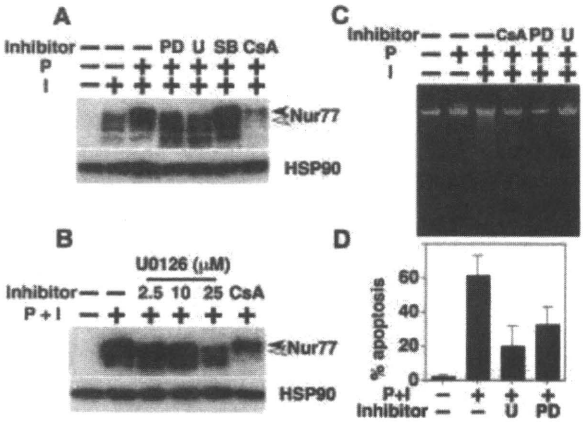


**Figure 2** Effects of MAPK inhibitors on Nur77 phosphorylation. (A) DO11.10 cells were pretreated with 50 μM PD98059 (PD), 10 μM U0126 (U), 10 μM SB203580 (SB) or 100 ng/ml CsA for 1 h, followed by stimulation with 5 ng/mL PMA (P) and 200 ng/mL A23187 (I) for 3 h. Cell lysates were subjected to immunoblot analysis with the anti-Nur77 mAb (upper panel) and an anti-HSP90 antibody as a loading control (lower panel). Solid and open arrowheads indicate mobility of the bands corresponding to hyper- and hypo-phosphorylated Nur77, respectively. (B) DO11.10 cells were pretreated with U0126 at the indicated concentrations or 100 ng/mL CsA for 1 h, followed by stimulation with 5 ng/mL PMA and 200 ng/mL A23187 (P + I) for 3 h. The cells were subjected to immunoblot analysis with the anti-Nur77 mAb (upper panel) and the anti-HSP90 antibody as a loading control (lower panel). (C) DO11.10 cells were pretreated with 50 μM PD98059 (PD), 10 μM U0126 (U) or 100 ng/mL CsA for 1 h, followed by stimulation with 5 ng/mL PMA (P) and/or 200 ng/mL A23187 (I) for 10 h. The cells were then subjected to DNA fragmentation assay. (D) DO11.10 cells were pretreated with 10 μM U0126 (U) or 50 μM PD98059 (PD) for 1 h, followed by stimulation with 5 ng/mL PMA and 200 ng/mL A23187 (P + I) for 16 h. The percentages of apoptotic cells were then evaluated by annexin-V staining. Three independent experiments were performed and data are presented as means ± SD.

cell activation was partially inhibited in the presence of a higher concentration (25 μM) of U0126, suggesting that an U0126-sensitive signaling pathway(s) is also involved in the Nur77 expression (Fig. 2B). As shown in Fig. 2C, DNA fragmentation, an indicator of apoptosis, caused by simultaneous stimulation with PMA and A23187 was blocked by the pretreatment of cells with CsA. Moreover, pretreatment with either U0126 or PD98059 also led to nearly complete inhibition of DNA fragmentation under conditions where the expression level of Nur77 was maintained at a level comparable to that without inhibitors. The suppressive effect of U0126 as well as PD98059 on DO11.10 was confirmed by FACS analysis using annexin-V as an indicator for apoptosis (Fig. 2D).

Although PD98059 and U0126 are highly selective inhibitors of the ERK1/2 signaling pathway (Pang *et al.* 1995; DeSilva *et al.* 1998), the ERK5 signaling pathway is also sensitive to these reagents (Kamakura *et al.* 1999). This was indeed the case with DO11.10 cells (Fig. 3). Pretreatment of the cells with PD98059 suppressed both ERK2 and ERK5 activation in response to PMA and A23187. Furthermore, U0126 reduced ERK2 and ERK5 activation to a nearly basal level (Fig. 3A,B). When we compared the kinetics of ERK1/2 and ERK5 activation, we found that ERK5 activation was more sustained in comparison with ERK2 (Fig. 3A,C). We also noted that stimulation with PMA and A23187 failed to activate ERK1 in DO11.10 cells where ERK1 was expressed to a level comparable to ERK2 (Fig. 3A and data not shown). On the other hand, CsA had no effect on ERK2 or ERK5 activation while apoptosis was inhibited.

These data raise the possibility that the ERK5 and/or ERK2 signaling pathways are involved in Nur77 phosphorylation. Consistent with this idea, we found that mouse Nur77 contains 12 potential MAPK phosphorylation sites, which are evolutionally conserved among mouse, rat and human species. Indeed, ERK5 as well as ERK2 directly phosphorylated recombinant mouse Nur77 protein *in vitro* (Fig. 3D). We thus examined whether ERK5 and/or ERK2 are able to phosphorylate Nur77 *in vivo* by using COS7 cells, which are resistant to Nur77-induced apoptosis, to avoid secondary effects caused by the apoptotic process. It is well established that MAPK is efficiently activated in the presence of its cognate upstream activator, MAPKK (Nishida & Gotoh 1993). The activation of either ERK2 (by co-transfection with ERK2 and ΔSESE, a constitutively active form of MEK1) or ERK5 (by co-transfection with ERK5 and MEK5(D), a constitutively active form of MEK5) led to Nur77 phosphorylation as demonstrated by the appearance of more slowly migrating bands (Fig. 3E). In contrast, the co-expression of inactive MEK1 (referred to here as SASA) and MEK5 (referred to here as MEK5(A)) failed to induce Nur77 phosphorylation. These results collectively indicate that ERK5 and ERK2 are capable of phosphorylating Nur77 *in vitro* and *in vivo*.

### ERK5-mediated phosphorylation is important for Nur77 function

We next examined whether MAPK-mediated phosphorylation affects Nur77 function. Previous reports have demonstrated that the translocation of Nur77 to mitochondria results in cytochrome *c* release, which causes activation of the caspase 9/caspase 3 cascade and leads to apoptosis in some cell lines such as LNCaP cells (Li *et al.*

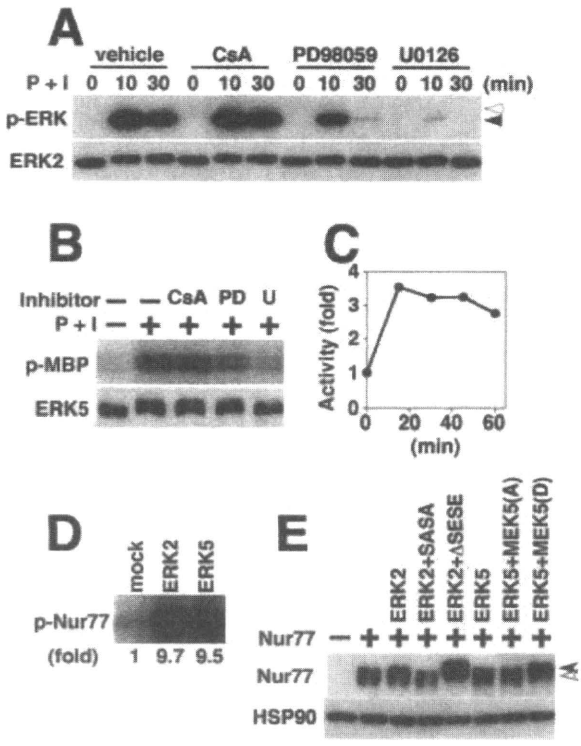


**Figure 3** ERK5 as well as ERK2 signaling pathways are involved in Nur77 phosphorylation. (A) DO11.10 cells were pretreated with 100 ng/mL CsA, 50 μM PD98059 or 10 μM U0126 for 1 h, followed by stimulation with 5 ng/mL PMA and 200 ng/mL A23187 (P + I) for the indicated times. ERK1/2 activity was estimated by immunoblot analysis with an anti-phospho-ERK1/2 mAb. Closed and open arrowheads indicate positions corresponding to phosphorylated ERK2 and phosphorylated ERK1, respectively. (B) DO11.10 cells were pretreated with 100 ng/mL CsA, 50 μM PD98059 (PD) or 10 μM U0126 (U) for 1 h, followed by stimulation with 5 ng/mL PMA and 200 ng/mL A23187 (P + I) for 10 min. The cell lysates were then subjected to immunoprecipitation with an anti-ERK5 antibody, followed by an *in vitro* kinase assay using MBP as a substrate. (C) DO11.10 cells were stimulated with 5 ng/mL PMA and 200 ng/mL A23187 for the indicated times. The cell lysates were immunoprecipitated with an anti-ERK5 antibody, and assayed for ERK5 activity. This experiments is a representative of two. (D) DO11.10 cells were stimulated with 5 ng/mL PMA and 200 ng/mL A23187 for 10 min, followed by immunoprecipitation with a control IgG (mock), the anti-ERK2 antibody, and the anti-ERK5 antibody. The immunoprecipitates were incubated with GST-Nur77 in the presence of [γ-$^{32}$P] ATP, and $^{32}$P incorporation was quantified on a BAS2000. (E) COS7 cells were transfected with an expression vector for GFP-fused Nur77 along with the indicated combination of MAPKK-MAPK. Cell lysates were obtained after 36-h incubation, and subjected to immunoblot analysis with an anti-GFP mAb (upper panel) and an anti-HSP90 antibody (lower panel). Closed and open arrowheads indicate Nur77 bands corresponding to a hyper-phosphorylated form and a hypo-phosphorylated form, respectively.

2000). However, TCR-induced Nur77 exclusively localized in the nucleus in DO11.10 cells (data not shown), which is consistent with a previous observation that the transcriptional activity of Nur77 correlated with its potential to cause apoptosis in T cells (Kuang *et al.* 1999). In addition, MAPK is known to translocate into the nucleus once activated (Cobb & Goldsmith 1995; Schaeffer & Weber 1999). It is thus likely that MAPK-mediated phosphorylation regulates the transcriptional activity of Nur77 in the nucleus. In fact, without MAPK-mediated phosphorylation, Nur77 had very low transcriptional activity whereas the activation of ERK5 pathway augmented the transcriptional activity of Nur77 (Fig. 4A). Interestingly, the activation of ERK2 pathway had a marginal effect on Nur77 activation. These data demonstrate that ERK5-mediated, but not ERK2-mediated phosphorylation is sufficient to activate Nur77. We also found that the activation of ERK5 pathway augmented A23187-induced apoptosis in DO11.10 cells (Fig. 4B). In addition, the expression of a dominant negative form of ERK5 (referred to here as dnERK5), which interferes the interaction between endogenous ERK5 and its substrate (Nakaoka *et al.* 2003), suppressed Nur77 activation induced by simultaneous stimulation with PMA and A23187 (Fig. 4C). It is thus likely that ERK5 plays a critical role in Nur77-mediated apoptosis, presumably through increasing transcriptional activity of Nur77. *In silico* analysis <http://mbs.cbrc.jp/research/db/TFSEARCH.html> suggests that Thr residue at 145 located within the transcriptional activation domain is a candidate for ERK5-mediated phosphorylation site. However, a mutant form of Nur77 where Ala was substituted for Thr 145 had similar transcriptional activity to wild-type Nur77 when over-expressed in DO11.10 cells (data not shown). The functional phosphorylation site(s) by ERK5 in Nur77 is now under investigation.

To examine whether the activation of ERK5 pathway is required for Nur77-induced apoptosis, we utilized a functional knockdown approach. Although Sohn *et al.* have reported the functional siRNA sequence for murine ERK5 (Sohn *et al.* 2005), we failed to reproduce their result via lentiviral vector-mediated introduction (data not shown). We thus chose more classical antisense approach to knockdown endogenous ERK5 in DO11.10 cells. Consistent with our expectation, the introduction of antisense ERK5 construct into DO11.10 cells reduced the expression level of endogenous ERK5, rendering the cells resistant to TCR-induced apoptosis (Fig. 4D, compare lanes 1 and 2). Furthermore, DO11.10 cells expressing dnERK5 were also resistant to TCR-induced apoptosis (Fig. 4D, compare lanes 2 and 3). We thus conclude that ERK5 is an essential component for Nur77-mediated T cell apoptosis.

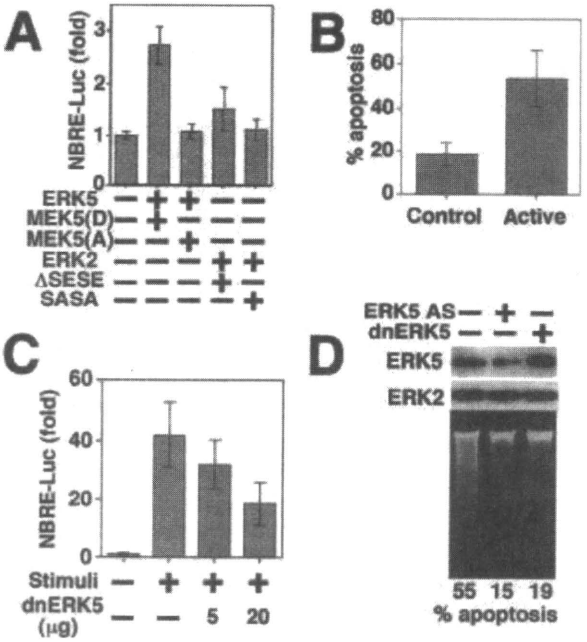


**Figure 4** ERK5-mediated phosphorylation of Nur77 is required to cause apoptosis. (A) DO11.10 cells were transfected with NBRE-luc and phRL-TK along with the indicated combination of MAPKK-MAPK. Luciferase activities were measured at 7 h after stimulation with 200 ng/mL A23187 according to the manufacturer's instructions (Promega). (B) DO11.10 cells were transfected with pEGFP alone (control) or MEK5(D) along with pEGFP-ERK5 (active). The cells were then stimulated with 200 ng/mL A23187 for 16 h. The percentages of apoptotic cells among GFP-positive cells were evaluated by annexin-V staining. Three independent experiments were performed and data are presented as means ± SD. (C) DO11.10 cells were transfected with NBRE-luc and phRL-TK along with or without the indicated amounts of the expression vector for dnERK5. Luciferase activities were measured at 7 h after stimulation with 5 ng/mL PMA and 200 ng/mL A23187. (D) DO11.10 cells were stably transfected with expression vectors for the indicated constructs. The expression level of ERK5 was indicated by immunoblot analysis with the anti-ERK5 antibody (upper panel) and the anti-ERK2 antibody served as loading control (middle panel). The transfectants were stimulated with plate-bound 145-2C11 for 12 h, and assayed for DNA fragmentation (lower panel). Shown are percentages of apoptotic cells evaluated by annexin-V staining at 16 h after stimulation.

## Discussion

ERK5, also known as BMK1, is a member of the MAPK family and is activated by a wide range of extracellular stimuli such as mitogens (Kato *et al.* 1997, 2000; English *et al.* 1999; Kamakura *et al.* 1999) and stress (Abe *et al.*

1996). It has been shown that ERK5 plays a critical role in a variety of physiological processes such as the differentiation of skeletal muscle cells, cardiac development, vascular maturation/angiogenesis and neural differentiation (Dinev *et al.* 2001; Regan *et al.* 2002; Nishimoto *et al.* 2005). However, whether ERK5 is involved in the TCR signaling pathway has been obscure. The results presented here suggest that the phosphorylation of Nur77 presumably mediated through ERK5 signaling pathway is required for its function in causing apoptosis during T cell activation. It is of interest to note that one of the best-characterized substrates of ERK5 is MEF2C (Kato *et al.* 1997), which has been shown to be involved in TCR-induced Nur77 induction (Youn *et al.* 1999). Consistently, the blockade of ERK5 activation with a higher dose of U0126 resulted in the partial inhibition of Nur77 expression during T cell activation (Fig. 2B). Furthermore, it has been reported that the C-terminal domain of ERK5 when over-expressed augments Nur77 gene expression (Kasler *et al.* 2000). These results collectively suggest that the ERK5 pathway affects Nur77 function through two distinct mechanisms, gene expression and post-translational modification.

We hypothesize that the ERK5–Nur77 pathway functions as a signal integrator to quantify the strength of TCR engagement and direct the cell fate of immature T cells determining whether or not the cells will die. This concept is in line with an observation that Nur77 is induced even during positive selection where a weak signal is transduced into the nucleus (Masuyama *et al.* 2001). Interestingly, it has been shown that the pretreatment of fetal thymocytes with PD98059 resulted in the blockade of negative selection, leading to the conclusion that ERK1/2 pathways are involved in negative selection (Mariathasan *et al.* 2000). However, based on our observation, this could be explained by the inhibition of Nur77 function through suppressing ERK5 pathway in PD98059-treated cells. Studies with conditional knockout mice recently established (Hayashi *et al.* 2004) will clarify the contribution of the ERK5 pathway to negative selection under physiological conditions.

It is yet to be determined why ERK2 activation had only a slight effect on the transcriptional activation of Nur77 although the activation of ERK2 pathway resulted in Nur77 phosphorylation to a level comparable to the ERK5 pathway (Fig. 3D,E). One possible mechanism is that ERK5 activation is sustained while ERK2 activation is transient and such sustained activation of ERK5 is required for the post-translational modification of Nur77 (Fig. 3A,C) as is the case for c-Fos stabilization during IL-6/gp130 stimulation (Sasaki *et al.* 2006). Alternatively, since ERK5 and ERK2 phosphorylate distinct subsets of transcription factors in the nucleus (Kamakura *et al.* 1999), it is possible that Nur77 phosphorylation mediated by ERK2, which may occur on a site(s) distinct from that phosphorylated by ERK5, rather inhibits Nur77 function. In accordance with this hypothesis, Katagiri *et al.* have reported that the activation of conventional Ras/MAPK cascade, which is presumably mediated through ERK1/2, resulted in the phosphorylation of Nur77 at Ser105, leading to nuclear export of Nur77 (Katagiri *et al.* 2000). This would be consistent with the observation demonstrating that the ERK1/2 pathway plays a critical role in positive selection (Sugawara *et al.* 1998): ERK1/2-mediated phosphorylation suppresses Nur77 function leading to survival and differentiation of DP cells.

In summary, present results show that ERK5 plays an important role in T cell apoptosis by enhancing the transcriptional activity of Nur77 through phosphorylation. Our results also suggest that ERK5 and ERK1/2 play distinct roles in the regulation of Nur77 and T cell fate during thymic development.

## Experimental procedures

### Cell culture and transfection

The DO11.10 mouse T-cell hybridoma (Haskins *et al.* 1983) and COS7 cells were maintained in RPMI 1640 medium containing 10% FCS, penicillin–streptomycin, 10 mM Hepes buffer solution and 50 μM β-mercaptoethanol (Invitrogen, Carlsbad, CA). For electroporation, DO11.10 cells ($1 \times 10^7$) suspended in Opti-MEM (Invitrogen) were mixed with 25 μg of plasmid DNA, and electroporated with a 250-V pulse at 960 μF on a Gene Pulser apparatus (Bio-Rad, Hercules, CA). COS7 cells were transfected with Superfect transfection reagent (Qiagen, Valencia, CA) according to the manufacturer's instructions.

### Antibodies and reagents

The antibodies and inhibitors used in this study include anti-Nur77 mAb (BD Bioscience, Franklin Lakes, NJ), anti-GFP mAb (Clontech, Palo Alto, CA), anti-ERK2 polyclonal antibody (Santa Cruz Biotechnology Inc., Santa Cruz, CA), anti-ERK5 polyclonal antibody and anti-αtubulin mAb (Sigma, St. Louis, MO), anti-phospho-ERK1/2 mAb and PD98059 (Cell Signaling, Beverly, MA), anti-HSP90 polyclonal antibody (Yonezawa *et al.* 1988), U0126 and SB203580 (Calbiochem, San Diego, CA). Anti-CD3ε mAb (145-2C11) was purified from the culture supernatant of a hybridoma 145-2C11. Phorbol-12-myristate 13-acetate (PMA) was purchased from Sigma, and calcium ionophore A23187 was from Calbiochem.

### Constructs

The Nur77 construct was provided by Dr B. A. Osborne (University of Massachusetts, Amherst, MA). An expression vector for

GFP-fused mouse Nur77 (pEGFP-Nur77) was constructed by subcloning a PCR fragment of Nur77 into the pEGFP-C1 vector (Clontech). A Nur77-responsive luciferase reporter plasmid (NBRE-luc) (Katagiri *et al.* 1997) was provided by Drs Y. Katagiri and G. Guroff (National Institutes of Health, Bethesda, MD). Expression vectors for MAPKs (pSRαHA-ERK2 and pSRαHA-ERK5) and MAPKKs (pSRαHA-SASA for a dominant-negative form of MEK1, pSRαHA-ΔSESE for a constitutively active form of MEK1, pSRα-MEK5(A) for a dominant-negative form of MEK5, and pSRα-MEK5(D) for a constitutively active form of MEK5) were provided by Dr E. Nishida (Kyoto University, Kyoto, Japan). Dominant negative ERK5 (referred to here as dnERK5), where Thr219 and Tyr221 were replaced with Ala and Phe, respectively, was generated by a PCR-based method and subcloned into pcDNA3.1 (Invitrogen). A cDNA fragment of mouse ERK5 was subcloned into pcDNA3.1 in a reverse direction to knockdown endogenous ERK5.

### *In vitro* kinase assay

Prior to the kinase assay for ERK5, DO11.10 cells were cultured in RPMI1640 containing 0.5% FCS for 4 h. After stimulation, cells were washed once with ice-cold PBS, and lysed in a lysis buffer solution (20 mM Tris–HCl, pH 7.5, 2 mM EGTA, 25 mM β-glycerophosphate, 1% Triton X-100, 2 mM dithiothreitol, 1 mM vanadate, 1 mM phenylmethylsulfonyl fluoride and 1% aprotinin), followed by centrifugation at 15 000 *g* for 30 min. The lysates were incubated for 2 h at 4 °C with an anti-ERK5 antibody along with protein A-Sepharose beads (Amersham Bioscience, Uppsala, Sweden). After washing 3 times with Tris-buffered saline containing 500 mM NaCl, the resulting immunoprecipitates were divided into two aliquots: one was used for the kinase assay, and the other for immunoblotting to evaluate the efficiency of immunoprecipitation. The immune complex was incubated at 30 °C for 30 min with a reaction buffer solution (20 mM Tris–Cl, pH 7.5, 10 mM $MgCl_2$ and 100 μM cold ATP along with 7.4 kBq of [γ-$^{32}$P]ATP) containing 10 μg of myelin basic protein (MBP) or GST-Nur77 as a substrate. In some experiment, GST-Nur77 was also incubated with the immunoprecipitates by an anti-ERK2 antibody. After SDS-PAGE, $^{32}$P incorporated into the substrate was quantified on an image analyzer (BAS2000, Fujifilm, Tokyo, Japan).

### DNA fragmentation assay

DNA fragmentation was detected as described previously (Hirt 1967). Briefly, DO11.10 cells ($1 \times 10^6$) were incubated at room temperature for 1 h in a fragmentation buffer solution (10 mM Tris–HCl, pH 8.0, 10 mM EDTA and 0.6% SDS). NaCl was then added to a final concentration of 1 M and the samples incubated at 4 °C overnight. Nuclear debris was then spun down for 30 min at 15 000 *g* at 4 °C. The DNA fraction in the supernatant was prepared by QIAquick PCR purification kit (Qiagen), followed by incubation with 200 μg/mL RNase A at 37 °C for 2 h. Samples were then electrophoresed on a 1.5% agarose gel and visualized by ethidium bromide staining.

### Annexin-V staining

After stimulation, DO11.10 cells were incubated with annexin-V-APC (BD Bioscience) in the presence of 1 mM $CaCl_2$ for 20 min at 4 °C, followed by washing with PBS containing 1 mM $CaCl_2$. Apoptotic cells were defined by APC-positive cells on a FACSCalibur.

### Luciferase assay

To examine the transcriptional activation of Nur77, we employed luciferase assay system using NBRE-luc as a reporter (Katagiri *et al.* 1997). DO11.10 cells were transiently co-transfected with expression vectors for MAPKK and MAPK along with NBRE-luc in combination with pRL-TK (Promega, Madison, WI) for normalization by electroporation at 250 V, 960 μF. Luciferase activities in cell lysates were measured in triplicate on a luminometer (LB9507; Berthold, Bad Wildbad, Germany), using the Dual-Luc assay system (Promega).

## Acknowledgements

We thank Dr L. K. Clayton for critical reading of the manuscript. This work was supported by a grant from the Mitsubishi Foundation, a Keio University Special Grant-in-Aid for Innovative Collaborative Research Project, a Grant-in-Aid for Scientific Research for young scientist (16790293 to S. M.) from the Japan Society for the Promotion of Science, a Grant-in-Aid for Scientific Research on Priority Areas (14021110 to S. K. and 16043248 to S. M.), a National Grant-in-Aid for the Establishment of a High-Tech Research Center in a private University, and a Scientific Frontier Research Grant from the Ministry of Education, Culture, Sports, Science and Technology of Japan.

## References

Abe, J., Kusuhara, M., Ulevitch, R.J., Berk, B.C. & Lee, J.D. (1996) Big mitogen-activated protein kinase 1 (BMK1) is a redox-sensitive kinase. *J. Biol. Chem.* **271**, 16586–16590.

von Boehmer, H. (2004) Stimulation of the T-cell receptor: receptor-controlled checkpoints in T-cell development. *Adv. Immunol.* **84**, 201–238.

van den Brink, M.R., Kapeller, R., Pratt, J.C., Chang, J.H. & Burakoff, S.J. (1999) The extracellular signal-regulated kinase pathway is required for activation-induced cell death of T cells. *J. Biol. Chem.* **274**, 11178–11185.

Calnan, B.J., Szychowski, S., Chan, F.K., Cado, D. & Winoto, A. (1995) A role for the orphan steroid receptor Nur77 in apoptosis accompanying antigen-induced negative selection. *Immunity* **3**, 273–282.

Chen, C.-Y., Del Gatto-Konczak, F., Wu, Z. & Karin, M. (1998) Stabilization of interleukin-2 mRNA by the c-Jun NH2-terminal kinase pathway. *Science* **280**, 1945–1949.

Cobb, M.H. & Goldsmith, E.J. (1995) How MAP kinases are regulated. *J. Biol. Chem.* **270**, 14843–14846.

DeSilva, D.R., Jones, E.A., Favata, M.F., Jaffee, B.D., Magolda, R.L., Trzaskos, J.M. & Scherle, P.A. (1998) Inhibition of mitogen-activated protein kinase kinase blocks T cell proliferation but does not induce or prevent anergy. *J. Immunol.* **160**, 4175–4181.

Diehl, N.L., Enslen, H., Fortner, K.A., Merritt, C., Stetson, N., Charland, C., Flavell, R.A., Davis, R.J. & Rincon, M. (2000) Activation of the p38 mitogen-activated protein kinase pathway arrests cell cycle progression and differentiation of immature thymocytes *in vivo*. *J. Exp. Med.* **191**, 321–334.

Dinev, D., Jordan, B.W.M., Neufeld, B., Lee, J.D., Lindemann, D., Rapp, U.R. & Ludwig, S. (2001) Extracellular signal regulated kinase 5 (ERK5) is required for the differentiation of muscle cells. *EMBO Rep.* **2**, 829–834.

English, J.M., Pearson, G., Hockenberry, T., Shivakumar, L., White, M.A. & Cobb, M.H. (1999) Contribution of the ERK5/MEK5 pathway to Ras/Raf signaling and growth control. *J. Biol. Chem.* **274**, 31588–31592.

Haskins, K., Kubo, R., White, J., Pigeon, M., Kappler, J. & Marrack, P. (1983) The major histocompatibility complex-restricted antigen receptor on T cells. I. Isolation with a monoclonal antibody. *J. Exp. Med.* **157**, 1149–1169.

Hayashi, M., Kim, S.W., Imanaka-Yoshida, K., Yoshida, T., Abel, E.D., Eliceiri, B., Yang, Y., Ulevitch, R.J. & Lee, J.D. (2004) Targeted deletion of BMK1/ERK5 in adult mice perturbs vascular integrity and leads to endothelial failure. *J. Clin. Invest.* **113**, 1138–1148.

Hirt, B. (1967) Selective extraction of polyoma DNA from infected mouse cell cultures. *J. Mol. Biol.* **26**, 365–369.

Hsu, H.C., Zhou, T. & Mountz, J.D. (2004) Nur77 family of nuclear hormone receptors. *Curr. Drug Targets Inflamm. Allergy* **3**, 413–423.

Kamakura, S., Moriguchi, T. & Nishida, E. (1999) Activation of the protein kinase ERK5/BMK1 by receptor tyrosine kinases. Identification and characterization of a signaling pathway to the nucleus. *J. Biol. Chem.* **274**, 26563–26571.

Kasler, H.G., Victoria, J., Duramad, O. & Winoto, A. (2000) ERK5 is a novel type of mitogen-activated protein kinase containing a transcriptional activation domain. *Mol. Cell. Biol.* **20**, 8382–8389.

Katagiri, Y., Hirata, Y., Milbrandt, J. & Guroff, G. (1997) Differential regulation of the transcriptional activity of the orphan nuclear receptor NGFI-B by membrane depolarization and nerve growth factor. *J. Biol. Chem.* **272**, 31278–31284.

Katagiri, Y., Takeda, K., Yu, Z.X., Ferrans, V.J., Ozato, K. & Guroff, G. (2000) Modulation of retinoid signaling through NGF-induced nuclear export of NGFI-B. *Nat. Cell Biol.* **2**, 435–440.

Kato, Y., Chao, T.H., Hayashi, M., Tapping, R.I. & Lee, J.D. (2000) Role of BMK1 in regulation of growth factor-induced cellular responses. *Immunol. Res.* **21**, 233–237.

Kato, Y., Kravchenko, V.V., Tapping, R.I., Han, J., Ulevitch, R.J. & Lee, J.D. (1997) BMK1/ERK5 regulates serum-induced early gene expression through transcription factor MEF2C. *EMBO J.* **16**, 7054–7066.

Koyasu, S., Suzuki, G., Asano, Y., Osawa, H., Diamantstein, T. & Yahara, I. (1987) Signals for activation and proliferation of murine T lymphocyte clones. *J. Biol. Chem.* **262**, 4689–4695.

Kuang, A.A., Cado, D. & Winoto, A. (1999) Nur77 transcription activity correlates with its apoptotic function *in vivo*. *Eur. J. Immunol.* **29**, 3722–3728.

Li, H., Kolluri, S.K., Gu, J., *et al.* (2000) Cytochrome *c* release and apoptosis induced by mitochondrial targeting of nuclear orphan receptor TR3. *Science* **289**, 1159–1164.

Liu, Z.G., Smith, S.W., McLaughlin, K.A., Schwartz, L.M. & Osborne, B.A. (1994) Apoptotic signals delivered through the T-cell receptor of a T-cell hybrid require the immediate-early gene nur77. *Nature* **367**, 281–284.

Mariathasan, S., Ho, S.S., Zakarian, A. & Ohashi, P.S. (2000) Degree of ERK activation influences both positive and negative thymocyte selection. *Eur. J. Immunol.* **30**, 1060–1068.

Mariathasan, S., Zakarian, A., Bouchard, D., Michie, A.M., Zuniga-Pflucker, J.C. & Ohashi, P.S. (2001) Duration and strength of extracellular signal-regulated kinase signals are altered during positive versus negative thymocyte selection. *J. Immunol.* **167**, 4966–4973.

Masuyama, N., Oishi, K., Mori, Y., Ueno, T., Takahama, Y. & Gotoh, Y. (2001) Akt inhibits the orphan nuclear receptor Nur77 and T-cell apoptosis. *J. Biol. Chem.* **276**, 32799–32805.

Nakaoka, Y., Nishida, K., Fujio, Y., Izumi, M., Terai, K., Oshima, Y., Sugiyama, S., Matsuda, S., Koyasu, S., Yamauchi-Takihara, K., Hirano, T., Kawase, I. & Hirota, H. (2003) Activation of gp130 transduces hypertrophic signal through interaction of scaffolding–docking protein Gab1 with tyrosine phosphates SHP2 in cardiomyocytes. *Circ. Res.* **93**, 221–229.

Nishida, E. & Gotoh, Y. (1993) The MAP kinase cascade is essential for diverse signal transduction pathways. *Trends Biochem. Sci.* **18**, 128–131.

Nishimoto, S., Kusakabe, M. & Nishida, E. (2005) Requirement of the MEK5–ERK5 pathway for neural differentiation in *Xenopus* embryonic development. *EMBO Rep.* **6**, 1064–1069.

Pang, L., Sawada, T., Decker, S.J. & Saltiel, A.R. (1995) Inhibition of MAP kinase kinase blocks the differentiation of PC-12 cells induced by nerve growth factor. *J. Biol. Chem.* **270**, 13585–13588.

Regan, C.P., Li, W., Boucher, D.M., Spatz, S., Su, M.S. & Kuida, K. (2002) Erk5 null mice display multiple extraembryonic vascular and embryonic cardiovascular defects. *Proc. Natl. Acad. Sci. USA* **99**, 9248–9253.

Rincon, M., Whitmarsh, A., Yang, D.D., Weiss, L., Derijard, B., Jayaraj, P., Davis, R.J. & Flavell, R.A. (1998) The JNK pathway regulates the *in vivo* deletion of immature CD4+CD8+ thymocytes. *J. Exp. Med.* **188**, 1817–1830.

Sakaue, M., Adachi, H., Dawson, M. & Jetten, A.M. (2001) Induction of Egr-1 expression by the retinoid AHPN in human lung carcinoma cells is dependent on activated ERK1/2. *Cell Death Differ.* **8**, 411–424.

Sasaki, T., Kojima, H., Kishimoto, R., Ikeda, A., Kunimoto, H. & Nakajima, K. (2006) Spatiotemporal regulation of c-Fos by ERK5 and the E3 ubiquitin ligase UBR1, and its biological role. *Mol. Cell* **24**, 63–75.

Schaeffer, H.J. & Weber, M.J. (1999) Mitogen-activated protein kinases: Specific messages from ubiquitous messengers. *Mol. Cell. Biol.* **19**, 2435–2444.